Studies on the regulation of *Photobacterium damselae* subsp. *piscicida* secreted proteins by the two-component system RstAB

Alexandre Jorge Julião Pinto
Master in Biochemistry
FCUP | ICBAS
2022

Supervisor
Ana do Vale, PhD, i3S

Co-supervisors
Jorge Azevedo, PhD, ICBAS, i3S
Johnny Lisboa, PhD, i3S


U.PORTO
ICBAS | INSTITUTO DE CIÊNCIAS BIOMÉDICAS ABEL SALAZAR
SCHOOL OF MEDICINE AND BIOMEDICAL SCIENCES

U.PORTO
FACULDADE DE CIÊNCIAS
UNIVERSIDADE DO PORTO

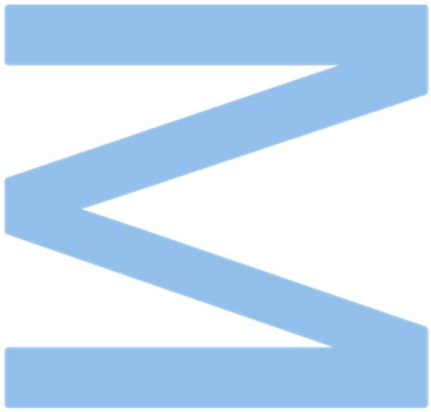

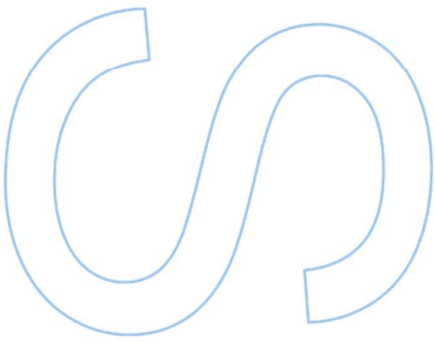

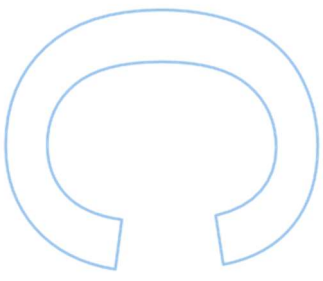

Sworn Statement

I, Alexandre Jorge Julião Pinto, enrolled in the Master's Degree in Biochemistry at the Faculty of Sciences and Institute of Biomedical Sciences Abel Salazar of the University of Porto hereby declare, in accordance with the provisions of paragraph a) of Article 14 of the Code of Ethical Conduct of the University of Porto, that the content of this dissertation reflects perspectives, research work and my own interpretations at the time of its submission.

By submitting this dissertation, I also declare that it contains the results of my own research work and contributions that have not been previously submitted to this or any other institution.

I further declare that all references to other authors fully comply with the rules of attribution and are referenced in the text by citation and identified in the bibliographic references section. This dissertation does not include any content whose reproduction is protected by copyright laws.

I am aware that the practice of plagiarism and self-plagiarism constitute a form of academic offense.

Alexandre Jorge Julião Pinto

28/09/2022, Porto

Acknowledgements

I would like to thank everybody in the Fish Immunology and Vaccinology Group from Instituto de Investigação e Inovação em Saúde (i3S) and Instituto de Biologia Molecular e Celular (IBMC), in particular to my supervisor doctor Ana do Vale, and co-supervisor doctor Johnny Lisboa. Thank you all for one more year under your tutelage, for the patience for all my short-comings, for pushing me to strive to be more than what was expected from me and for giving me the opportunity to continue the project I started in my Bachelor's degree, in order to conclude my master degree in Biochemistry.

To my co-supervisor doctor Jorge Azevedo from the Organelle Biogenesis and Function Group from i3S and IBMC, for all the feedback and guidance in the hurdles that I encountered during this project.

I would also like to thank the support from the Biochemical and Biophysical Technologies (protein quantification and purification and circular dichroism) and from the Cell Culture and Genotyping (thermal shift and RT-qPCR) scientific platforms of i3S (Porto, Portugal)

To my family, for all the support, words of wisdom and love, that you have always given me. Without those, I would not have been able to persevere through all the hardships in this journey that were my study years so far.

To my girlfriend Mariana, for all the love and attention, all the motivation, the late night calls and your patience.

To my friends, the family that I chose, Bruno, Varela, Luís, Munhoz, Ariana, Rebeca, Rute, Daniela, Leonor, Catarina, Beatriz, Ana. Some of you started this journey with me, some entered mid-journey, but all of you made it exponentially better.

This work was financed by FEDER - Fundo Europeu de Desenvolvimento Regional funds through the COMPETE 2020 - Operacional Program for Competitiveness and Internationalization (POCI), Portugal 2020, and by Portuguese funds through FCT - Fundação para a Ciência e a Tecnologia, I.P., in the framework of the project POCI-01-0145-FEDER-030018 (PTDC/CVT-CVT/30018/2017). It was also financed by FCT— Fundação para a Ciência e a Tecnologia, I.P., in the framework of the project PTDC/CVT-CVT/7177/20.

Resumo

Photobacterium damselae subsp. *piscicida* (*Phdp*) é uma bactéria Gram-negativa que infecta várias espécies de peixes marinhos. A toxina apoptogénica AIP56 e a toxina binária PBT têm sido implicadas na virulência de *Phdp*. Adicionalmente, foi sugerido que a hidrolase de peptidoglicano PnpA pode conferir a esta bactéria uma vantagem competitiva contra bactérias com que partilha o habitat. Contudo, nada se sabe da regulação da expressão destes fatores. Os sistemas de dois componentes (TCSs), que compreendem um sensor histidina quinase que transmite um sinal para um regulador de resposta, regulam a expressão de fatores de virulência e controlam a resistência a antibióticos em várias bactérias. Em particular, o RstAB TCS, recentemente descoberto em *Phdp*, demonstrou ser um regulador da virulência em *Photobacterium damselae* subsp. *damselae*, embora nada se saiba sobre o seu papel na regulação da virulência nesta espécie. Neste trabalho, foi investigado o papel do RstAB como regulador da virulência da *Phdp*. Usando um mutante de deleção *rstB* (*ΔrstB*), produzido anteriormente a partir da estirpe MT1415 de *Phdp*, e a estirpe complementada correspondente (*ΔrstB*+p*rstB*), a virulência das estirpes WT, *ΔrstB* e *ΔrstB*+p*rstB* para robalo foi comparada. Foi, assim, possível demonstrar que a virulência da estirpe *ΔrstB* está fortemente atenuada, quando comparada com a das estirpes WT e *ΔrstB*+p*rstB*. A análise por RT-qPCR e SDS-PAGE de sobrenadantes de cultura mostrou que a deleção de *rstB* levou a uma drástica diminuição na expressão de AIP56, PBT e PnpA, quer a nível do mRNA, quer a nível proteico. Esta análise também revelou que o RstB regula a expressão de OMP19, uma proteína da membrana externa muito abundante recentemente identificada. Também avaliamos se o RstB regula a expressão das adesinas triméricas autotransportadas PadA e PadB, recentemente identificadas num isolado de campo *Phdp*, e revelamos que RstB regula a expressão de PadA, mas não de PadB. De seguida, foi investigada a capacidade do RstA de se ligar às regiões promotoras dos genes *aip56*, *pnpA*, *pbt, omp19, padA e padB*. Electrophoretic Mobility Shift Assays (EMSAs) mostraram que o RstA recombinante interage diretamente com essas regiões promotoras. Além disso, os principais resíduos envolvidos nesta interação foram identificados, através de mutagénese dirigida e EMSA. Em conjunto, os dados obtidos sugerem que a via canónica do RstAB TCS regula positivamente a expressão dos genes *aip56*, *pnpA*, *pbt*, *omp19* e *padA*, e apontam para o envolvimento de mecanismos cross-talk na regulação da expressão de *padB* por RstA.

Palavras-chave: Sistema de dois componentes, RstAB, *Photobacterium damselae* subsp. *piscicida*, AIP56, Fatores de Virulência, Virulência

Abstract

Photobacterium damselae subsp. *piscicida (Phdp)* is a Gram-negative bacterium that infects several marine fish species. The apoptogenic toxin AIP56 and the binary toxin PBT have been implicated in *Phdp* virulence. Additionally, it has been suggested that the peptidoglycan hydrolase PnpA may confer to *Phdp* an advantage against putative competitor bacteria, however nothing is known about the expression regulation of these factors. Two component systems (TCSs), which are comprised of a sensor histidine kinase that transmits a signal to a response regulator, regulate the expression of virulence factors and control antibiotic resistance in various bacteria. In particular, the RstAB TCS has been shown to be a master regulator of virulence in *Photobacterium damselae* subsp. *damselae* and has recently been discovered in *Phdp*, although nothing is known about its role in this subspecies. In this work, the role of RstAB as a regulator of *Phdp* virulence was investigated. Using an *rstB* deletion mutant (Δ*rstB*) previously produced using MT1415 as background and the correspondent complemented strain (Δ*rstB*+p*rstB*), the virulence of the WT, Δ*rstB* and Δ*rstB*+p*rstB* for sea bass was compared, showing that Δ*rstB* is strongly impaired in virulence, when compared to the WT and Δ*rstB*+p*rstB* strains. RT-qPCR and SDS-PAGE analysis of culture supernatants showed that deletion of *rstB* led to a strong decrease in the expression of AIP56, PBT and PnpA at mRNA and protein levels. These analysis also revealed that RstB regulates the expression of OMP19, a newly identified and very abundant outer membrane protein. We also evaluated if RstB regulates the expression of the recently identified PadA and PadB trimeric autotransporter adhesins, which were identified in a field isolate of *Phdp*, and revealed that RstB regulates the expression of PadA but not PadB. Next, the ability of RstA to bind to the promoter regions of *aip56*, *pnpA*, *pbt*, *omp19*, *padA* and *padB* was investigated. Electrophoretic Mobility Shift Assays (EMSAs) showed that recombinant RstA directly interacts with these promoter regions. Furthermore, key residues important for this interaction were identified by combining site-directed mutagenesis with EMSA. Altogether, these data suggest that the canonical RstAB pathway positively regulates *aip56*, *pnpA*, *pbt*, *omp19* and *padA* expression, and point to the involvement of a cross-talk mechanism in the regulation of *padB* expression by RstA.

Keywords: Two-component systems, RstAB, *Photobacterium damselae* subsp. *piscicida*, AIP56, Virulence Factors, Virulence

Table of Contents

List of Tables

List of Figures

List of Abbreviations

A

AIP56 – Apoptosis Inducing Protein of 56 kDa

ABC – ATP-Binding Cassette

APEC – Avian Pathogenic *E. coli*

APS – Ammonium persulfate

AI-2 –Autoinducer-2

B

BSA – Bovine Serum Albumin

C

Cam – Chloramphenicol

CFU – Colony-Forming Unit

D

DvLysin – *Desulfovibrio vulgaris* lysin

Dly – Damselysin

DTT – Dithiothreitol

E

E. coli – *Escherichia coli*

ECPs – Extracellular Products

EPEC – Enteropathogenic *E. coli*

EDTA – Ethylenediaminetetraacetic acid

F

FIV – Fish Immunology and Vaccinology

G

GLB – Gel Loading Buffer

I

ITC – Isothermal Titration Calorimetry

IPTG – Isopropyl β-D-1-thiogalactopyranoside

IMAC – Immobilized Metal Ion Affinity Chromatography

K

Kan – Kanamycin

L

LB – Luria-Bertani broth

M

MT1415Rif^{R} – MT1415 strain with rifampicin resistance

O

OD – Optical Density

ON – Overnight

OMP19 – Outer membrane protein of 19 kDa

P

Phdp – *Photobacterium damselae* subsp. *piscicida*

PI3K – Phosphoinositide 3-kinase

PBT – Photobacterium Binary Toxin

PnpA - *Photobacterium* NlpC-like protein A

PCR – Polymerase Chain Reaction

PadA – *Photobacterium* adhesin A

PadB – *Photobacterium* adhesin B

PTM – Post-translational modification

Phdd – *Photobacterium damselae* subsp. *damselae*

PhlyP – Phobalysin P

PhlyC – Phobalysin C

R

RT-PCR – Reverse Transcription-Polymerase Chain Reaction

RT-qPCR – Real Time-quantitative Polymerase Chain Reaction

RR – Response Regulator

Δ*rstB* – *Phdp* MT1415 deletion mutant for *rstB*

Δ*rstB*+*prstB* – *Phdp* MT1415 Δ*rstB* complemented with plasmid-encoded *rstB*

rpm – Rotations per minute

Rif – Rifampicin

RT – Room Temperature

S

SEC – Size Exclusion Chromatography

SK – Sensor Histidine Kinase

SPI-1 – *Salmonella* pathogenicity island-1

SPI-2 – *Salmonella* pathogenicity island-2

T

T2SS – Type II Secretion System

TBDT – TonB-dependent transporter

TAA – Trimeric Autotransporter Adhesin

T3SS – Type III Secretion System

TCS – Two-Component regulatory System

TSA-1 – Tryptic Soy Agar with 1% NaCl

TSB-1 – Tryptic Soy Broth with 1% NaCl

TCA – Trichloroacetic acid

TEMED – Tetramethylethylenediamine

TAE – Tris-Acetate-EDTA buffer

T4 PNK – T4 polynucleotide kinase

TEP – Thienopyridine

W

WT – Wild Type

1. Introduction

1.1 *Photobacterium damselae* subsp. *piscicida*

Aquaculture has been playing an ever-increasing role in food production and has currently a central role as a supplier of healthy fish products to the exponentially growing world population [1]. Bacterial infections are one of the main concerns that threaten aquaculture production, due to their negative impact on productivity, which often leads to significant economic losses [2]. *Photobacterium damselae* subsp. *piscicida* (*Phdp*) is a Gram-negative bacterium of the Vibrionaceae family that infects several species of warm water marine fish and is responsible for multiple infections reported not only in aquaculture environments but also in the wild [3]. *Phdp* was first detected in Chesapeake Bay [4], after reports of a massive fish kill. It was dubbed *Pasteurella piscicida* but was later reclassified and named *Photobacterium damselae* subsp. *piscicida* [5]. Cases of infection by this pathogen have been reported across many species and geographical locations [6]. Mortality rates are affected by age, as it has been reported that infection of larvae or juvenile fishes can lead to 90-100% mortality, whereas adult fish (over 50 g of weight) show a higher degree of resistance [7]. The widespread distribution of *Phdp*, combined with its capability to resist antibiotics and the lack of efficient vaccination strategies capable of preventing the infection, have led to the recognition of this pathogen as a great threat to mariculture [8].

The first external signs of fish infection by *Phdp* are skin discoloration and scattered petechiae in the abdominal area. With the progression of the infection, the fish start presenting lethargy and a loss of equilibrium, typical signs of a moribund fish [9]. Analysis of infected tissues revealed the presence of *Phdp* in organs associated with the immune response, like the spleen and the head-kidney, as well as in the bloodstream [9]. Infected tissues contain not only high numbers of bacteria, but also many apoptotic cells and apoptotic bodies as well as lysing cells and cell debris, indicating that the disease associated with *Phdp* infection culminates in generalized bacteraemia and widespread tissue necrosis [9].

1.2 *Phdp* virulence factors/mechanisms

1.2.1 Extracellular products

Many bacterial fish pathogens secrete a variety of extracellular products (ECPs) [10] that often play a role in virulence, either by facilitating bacterial nutrition or by counteracting the host immune response [10]. It was known for long that ECPs from *Phdp* were lethal to many fish species [11] but, for many years, the specific ECPs components responsible for the observed toxicity remained unidentified. In 2005, do Vale and colleagues identified AIP56, a 56 kDa apoptosis inducing protein secreted by *Phdp* [6] that leads to the apoptosis of host macrophages, compromising the immune response [12]. This toxin, which is secreted via a type II secretion system (T2SS) [13] is currently the best characterized virulence factor of *Phdp* and might be one of the major players contributing for the toxicity of the ECPs. It is an AB type toxin [14] that comprises a catalytic A component and a delivery B component that is responsible for the binding to host cells and delivery of the catalytic component into the host cell's cytosol through a mechanism triggered by low-endosomal pH [15]. Once at the cytosol, the catalytic component cleaves the REL homology domain of the p65 subunit of NF-kB at a specific site. This impairs NF-kB-DNA interaction and compromises NF-kB activity, culminating in cell apoptosis [14]. Interestingly, not all AIP56 is delivered into the cytosol [15]. In fact, it has been shown that a fraction of the endocytosed toxin enters a recycling pathway dependent on phosphoinositide 3-kinase (PI3K) activity and is excreted back into the extracellular medium [15] (Figure 1).

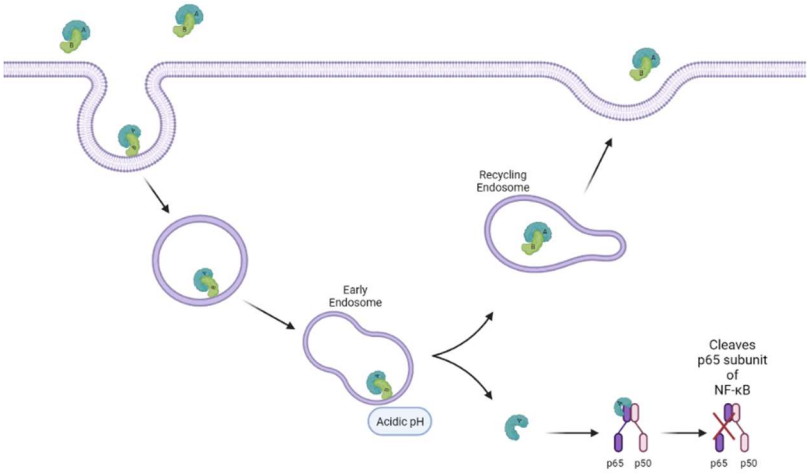

Figure 1 – Schematic representation of the intracellular routes used by AIP56. AIP56 is an AB type toxin that comprises an A component with catalytic activity linked to a delivery B component. Upon reaching early endosomes, the decrease in pH triggers the translocation of a pool of AIP56 into the cytosol, leading to the cleavage of NF-κB p65. A pool of endocytosed toxin returns to the extracellular compartment by following the recycling pathway. Image created with BioRender.com.

Recent work developed at the Fish Immunology and Vaccinology (FIV) group of IBMC/i3S has also allowed for the identification of the binary toxin PBT (*Photobacterium* Binary Toxin) that is structurally similar to the PirAB toxin from *Vibrio parahaemolyticus* [16]. PBT is a secreted toxin composed by PBTa (~11 kDa) and PBTb (~60 kDa) and, similarly to AIP56, is highly toxic to host macrophages (Unpublished data from FIV Group). Although this toxin is lethal to fish and is required for full virulence of *Phdp*, the mechanisms by which it kills macrophages have not yet been characterized.

Another recently identified secreted factor of *Phdp* is PnpA (*Photobacterium* NlpC-like protein A), a type II secreted 55 kDa peptidoglycan hydrolase with a four-domain structure, that shows similarity with *Desulfovibrio vulgaris* lysin (DvLysin) and has an affinity to the γ-D-glutamyl-*meso*-diaminopimelic acid bond in peptidoglycans [17]. This hydrolase is unable to cleave peptidoglycan from most bacteria but degrades the peptidoglycan from *Vibrio anguillarum* and *Vibrio vulnificus*. Although virulence assays conducted using a *Phdp pnpA* knockout strain showed no changes in virulence after *pnpA* deletion, it has been proposed that PnpA may confer a competitive advantage to *Phdp*, by targeting bacteria that grow in the same environment and may compete with *Phdp* for nutrients [17].

1.2.2 Iron acquisition systems

Iron (Fe) is an essential co-factor for many cellular processes in almost all organisms [18]. However, this micronutrient has low bioavailability and can be toxic in high concentrations [18]. As such, the levels of iron present in all cells are strictly regulated [18]. Hosts developed strategies to restrict the iron available to the pathogen, by depleting the ions present in the infection site [19]. In response, many pathogens developed highly efficient iron acquisition systems [20]. The best known strategies are the synthesis of high-affinity iron-binding siderophores, which are low molecular weight molecules capable of chelating iron, allowing its transport to the bacteria [21] and the acquisition of iron from heme groups [22, 23]. Both systems utilize active transport in order to transport iron-binding molecules to the interior of the cell. Many Gram-negative bacteria utilize the outer membrane TonB-dependent transporters (TBDT) to transport the Fe(III)-siderophore or the heme for this purpose [24]. TBDT proteins contain a conserved N-terminal domain (TonB box) that mediates interaction with TonB, which transduces the energy required for the transport of these molecules [25]. After the heme or Fe(III)-bound siderophores are transported to the periplasm, specific periplasmic proteins bind to them and deliver them to specific ATP-driven ABC (ATP-binding cassette) transporters present in the cytoplasmic membrane [26]. These catalyze the

transport to the cytoplasm of the iron binding molecules, where the Fe(III) is released by a reduction step, allowing the aposiderophores to be reutilized, i.e., re-exported to the extracellular medium [24] (Figure 2). On the contrary, after transport to the inner membrane, heme is degraded in order to release iron, as well as to reduce the probability of formation of toxic free iron radicals. This is achieved by heme oxygenases, present in the cytoplasm [27], which can be from one of three families, HO-1 heme oxygenases, Chuz heme oxygenases, and IsdG/I heme oxygenases [22].

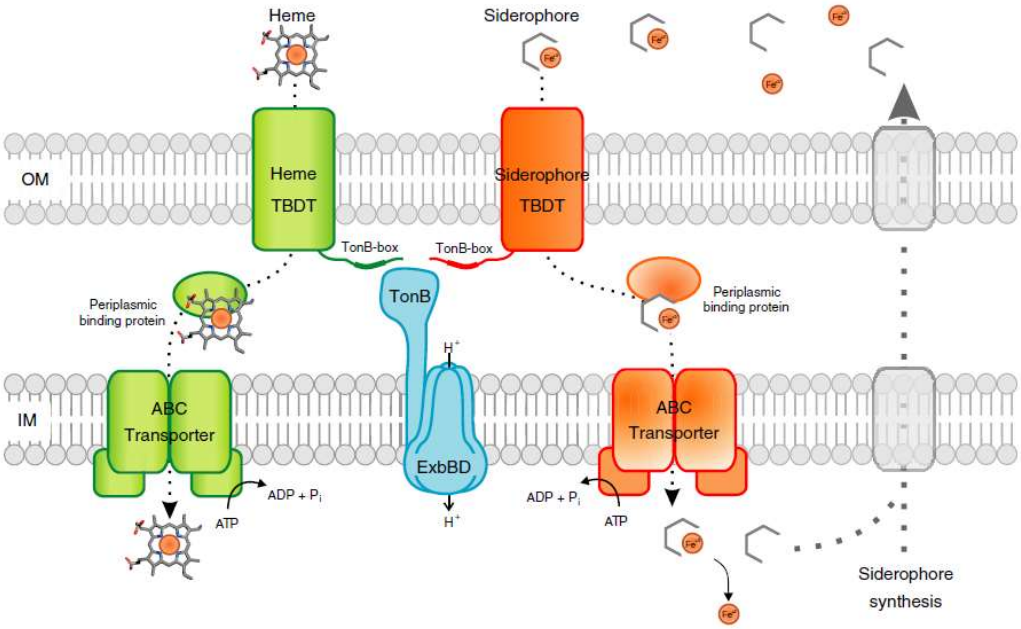

Figure 2 – Iron uptake systems in Gram-negative bacteria. Heme and siderophore bound Fe (III) is transported via TonB-dependent transporters (TBDT) present in the outer membrane (OM) to the periplasm, where specific periplasmic binding proteins will direct them to inner membrane (IM) bound ATP-binding cassette transporters (ABC), which mediate their transport to the cytoplasm. At the cytoplasm, heme and siderophores release Fe(III) via reduction, and aposiderophores can be reutilized, whereas heme gets degraded. Image from [24].

Phdp has been shown to synthesize a high-affinity iron-binding siderophore called piscibactin [28]. This siderophore is similar to yersiniabactin, produced by *Yersinia* sp., and is located in the pathogenicity island *irp*-HPI, encoded in the pPHDP70 plasmid [21, 29, 30]. This plasmid and its encoding siderophore, are essential for *Phdp* survival and virulence, as it was demonstrated that deletion of this plasmid or mutation of piscibactin biosynthesis genes leads to impaired growth in low iron concentration media and impaired virulence in fish [28, 29]. Magariños et *al.*, showed that the presence of hemin or hemoglobin, two sources of heme groups, prior to injection of *Phdp*, increases its lethality [31]. Furthermore do Vale et *al.,* demonstrated that *Phdp* can grow in iron-limited media, if hemin is added to the media [31]. More recently, reverse transcription-polymerase chain reaction (RT-PCR), has allowed to uncover that the *hut*CD genes, which encode the ABC transporter, are present in *Phdp*, are expressed during infection and can be detected in infected fish tissues [32]. This transporter, which is responsible

for transporting heme across the inner membrane, has been shown to be essential for hemin utilization [32].

1.2.3 Capsular polysaccharides and host cell adhesion mechanisms

Colonization of host is essential for bacterial pathogenesis [33]. It often involves the evasion/counteraction of host immune responses, adherence to target cells and host cell invasion [33]. Bacteria have developed many strategies to achieve these steps. Many bacterial cells possess capsular polysaccharide layers with variable structures and functions that are implicated in virulence [34]. The roles of capsules include resistance to antimicrobial action [35], masking antigenic determinants present at the bacterial surface [36] or mimicking host antigens, “disguising” the bacteria as a host-cell [37].

A study conducted by Bonet et *al*., showed that *Phdp* produces capsular polysaccharides, and that the virulent strains of *Phdp* present a capsule [38]. It has been demonstrated that the presence of capsular polysaccharides increases the bacterial resistance to the bactericidal action of fish serum and is essential for virulence in fish [39]. It has been proposed that the increased virulence of the capsulated bacteria may be due to an indirect increase in invasion of host cells, since more bacteria survive the antimicrobial action of serum, leading to increased cell invasion [40].

A crucial step for successful bacterial infection is adhesion to host cells and tissues [41]. This can be achieved by bacterial proteins of varying degrees of complexity known as adhesins [41], commonly grouped into fimbrial and non-fimbrial [42]. Fimbrial adhesins, which include fimbriae or pili, are polymeric structures present in the surface of Gram-negative and Gram-positive bacteria, that play a role in adhesion, motility, DNA transfer and biofilm formation [41, 43]. On the other hand, non-fimbrial adhesins are monomeric or trimeric proteins that also participate in adhesion [44]. Autotransporter (AT) adhesins are one of the principal classes of non-fimbrial adhesins [45]. They belong to the AT superfamily of proteins and play a major role in virulence, often by mediating host cell adhesion [43].

In Gram-negative bacteria, autotransporter proteins are more commonly secreted by the type V secretion system and include four common structural elements: 1) a signal peptide located in the N-terminal region that plays a role in transport across the inner membrane; 2) the functional component, also known as the passenger domain; 3) a linker region of varying size; and 4) a translocation domain [46, 47] (Figure 3A). The translocation domain presents a characteristic β-barrel structure that will become embedded in the outer membrane and is required for delivery of the passenger domain to the cell surface [48]. The first step in this secretion system requires the SEC

translocase complex, in order to translocate the autotransporter protein across the inner membrane [49]. There are five subtypes of the type V secretion system (Va-Ve), according to the structures present in the outer membrane [47].

Phdp displays glycoprotein-mediated adherence to fish intestines [50] and is capable of entering non-phagocytic cells via an actin-dependent mechanism that takes advantage of the cell metabolism [51]. Although it is reasonable to speculate that these adhesive properties of *Phdp* may be essential for successful infection, to date, the bacterial factors mediating the *Phdp* adherence have not been identified. Recently, two trimeric autotransporter adhesins (TAAs) have been identified in a *Phdp* field isolate (Unpublished data from FIV Group) (Figure 3B). These adhesins were named PadA and PadB (for *Photobacterium* adhesin A and B, respectively). PadA and PadB are absent in most laboratory strains of *Phdp* and, although it is likely that they play a role in virulence, nothing is currently known about their modes of action or the mechanisms that regulate their expression during infection. *In silico* analysis revealed that PadA and PadB belong to the Vc subtype of autotransporters, which is characterized by a trimeric passenger domain, presenting a stalk, neck and β-helical head region connected to a β-barrel anchored to the outer membrane [52, 53] (Figure 3B).

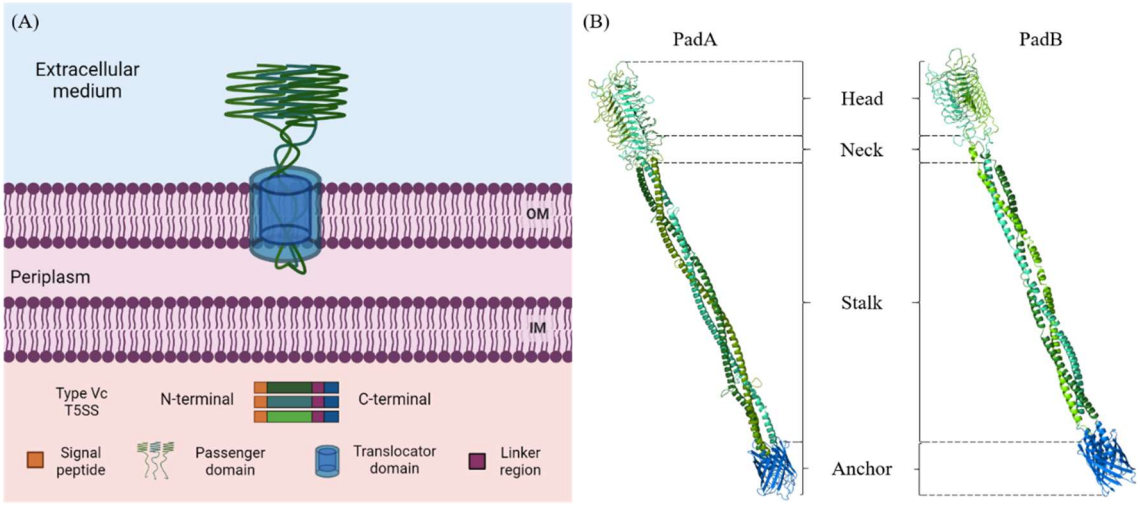

Figure 3 – *Photobacterium damselae* subsp. *piscicida* secretes two trimeric autotransporter adhesins. (A) Schematic representation of the trimeric autotransporter adhesins or Vc secretion system. The trimeric autotransporter adhesins contain the four common domains of a T5SS. These are a signal peptide located in the N-terminal region (orange), the functional component also known as the passenger domain (varying green), a linker region of varying size (purple), and finally a translocation domain anchored in the outer membrane (blue). Image adapted from [43] and created with BioRender.com. **(B)** Model of the three-dimensional structure of PadA and PadB from *Photobacterium damselae* subsp. *piscicida*. Same color code as in (A). PadA and PadB model was generated using modeller program [54] based in YadA structure.

1.2.4 Type III secretion system

Type III secretion systems (T3SS) or injectisomes are virulence-associated secretion systems, present in many Gram-negative bacteria, such as enteropathogenic *E. coli* (EPEC), *Salmonella* and *Pseudomonas aeruginosa* [55], that allow the injection of effector proteins directly into target eukaryotic cells [56]. They are membrane-embedded protein complexes, with a molecular weight of approximately 6 MDa, comprised by approximately 20 different proteins (Box 1), with varying copy numbers [57]. T3SS have the ability to sense host-cell contact, triggering the injection of effector proteins through translocation pores assembled in target cell membrane [58].

Box 1

Injectisomes are comprised of approximately 20 different proteins, with varying names according to the bacteria [59]. These proteins can be divided according to their function in the injectisome into base components, cytoplasmic components, export apparatus and filament formation, needle tip components and translocon [56]. The base anchors the T3SS to the bacterial inner membrane and is composed by three proteins, SctC, SctD and SctJ [56]. The cytoplasmic components are SctK, SctQ, SctL, SctN and SctO and can exist both in T3SS-bound form or in a free cytoplasmic complex [60]. SctN acts as an ATPase [61] and SctO connects SctN with the major export apparatus protein SctV [62]. Besides SctV, the export apparatus is comprised of four other proteins, SctR, SctS, SctT and SctU [63]. The helical needle used to inject effector proteins in target cells is comprised of more than 100 copies of SctF [64]. The needle tip is comprised of a pentameric hydrophilic translocation protein named SctA [64] and is associated with a translocon complex formed by the hydrophobic translocation proteins, SctB and SctE responsible by host-cell penetration [58]. SctW is a “gate-keeper” protein, responsible for late substrate secretion, after host-cell sensing by the needle tip [65, 66].

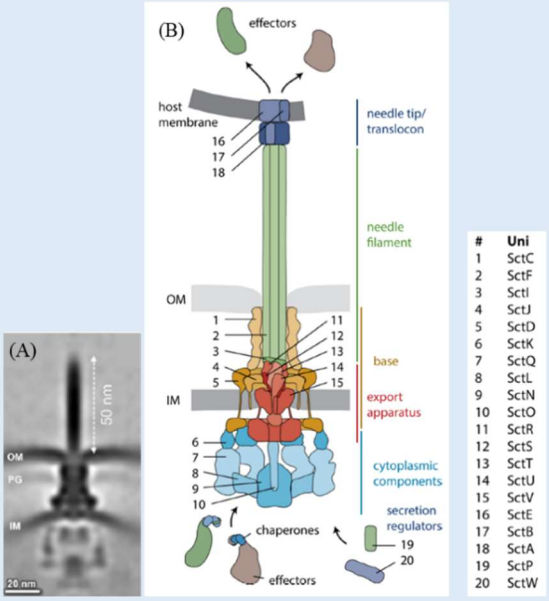

Figure 4 – Structure of a T3SS. (A) *In situ* structure of host-free injectisome of *Salmonella typhimurium* obtained by cryo-eletron tomography. Adapted from [58]. **(B)** Schematic representation of a T3SS. Different components are numbered and each color represents a structural subunit. Nomenclature presented is the unified nomenclature proposed in [59]. Image adapted from [56]. Abbreviations: OM - outer membrane, IM – inner membrane, PG – peptidoglycan.

In *Phdp*, this secretion system was first identified in 2019, in two strains, PP3 and SNW-8.1 [67]. However, a study conducted in 2020 showed that the T3SS is highly prevalent in many *Phdp* strains collected from varying hosts and geographical locations, going as far back as 1980 [68]. Recently, it has been reported that the *Phdp* T3SS is encoded in a highly-unstable, virulence-associated plasmid entitled pPHDPT3 [69], which also encodes PadA and PadB. The pPHDPT3 instability *in vitro* likely explains why PadA, PadB and *Phdp* T3SS remained unidentified for so long. The discovery of pPHDPT3 and its *in vitro* instability led the authors to propose that *Phdp* virulence may have been underestimated, due to the loss of pPHDPT3 in laboratory *Phdp* strains [69].

1.3 Two-component regulatory systems

Two-component regulatory systems (TCSs) are signal transduction pathways used in bacteria and archaea, as well as in some eukaryotic organisms like plants. They respond to changes in environmental conditions and play major roles in survival, virulence and cell growth [70]. In response to environmental stimuli, TCSs lead to altered gene expression, either repression or activation, and in some instances, to changes in biochemical activities of certain proteins [71]. TCS can be categorized according to their complexity (Box 2). Basic TCS consist of a sensor histidine kinase (SK), which usually presents as an homodimer, which detects environmental alterations (such as changes in pH or salt concentration or antimicrobial peptides) and a response regulator (RR) that modulates gene expression [72]. Signal transduction by TCSs occurs via a cascade of phosphorylation/dephosphorylation reactions [73]. The signal is transferred from one component to the other via a phosphorelay, that begins in the sensor kinase, in which a conserved histidine residue is autophosphorylated upon detection of a specific stimulus, leading to a conformational change of the ATP-binding domain, that allows the transfer of a phosphoryl group from ATP [74, 75]. The phosphoryl group in the sensor kinase is then transferred to a conserved aspartate residue on the response regulator [74], leading to its dimerization. It has been proposed that binding of the activated response regulator to DNA occurs in a sequential manner: a monomer binds to DNA and leads to a conformational change on the second monomer, facilitating its binding to DNA and increasing the binding affinity [73]. The sensor kinase also has phosphatase activity, which allows it to remove the phosphate from the response regulator to quickly reset the system [75] (Figure 5).

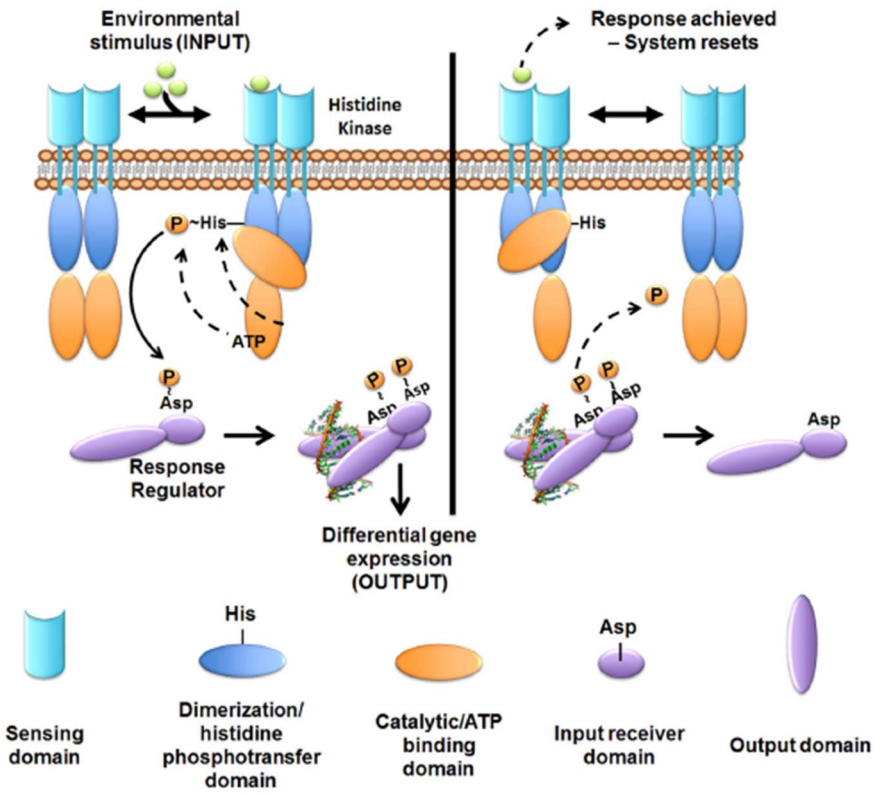

Figure 5 – Representation of the stimulus response of a basic two-component regulatory system. The environmental stimulus binds to sensor histidine kinase (SK) in the sensor domain (light blue), leading to conformational change of the ATP binding domain (orange) which catalyzes the transfer of a phosphoryl group from ATP to the quorum sensing-like domain of the response regulator (RR) (purple). The transfer of the signal via phosphorelay allows for the formation of an RR dimer that will then bind to the target promoter DNA, regulating gene expression. After gene expression, the phosphoryl group is transferred back to the SK, resetting the system. Image adapted from [75].

The fact that there are multiple phosphorylated intermediates is an advantage, as it allows for many checkpoints to abort the phosphorelay when necessary [75].

These phosphorylation/dephosphorylation reactions are tightly regulated, as they must be fast enough to guarantee that the response is synchronized, even when the stimulus is fluctuating, but also slow enough to remain after the system has begun its activation [74].

Although TCSs present a high degree of specificity, they often cross-talk with each other in different steps of signal transduction. Firstly, cross-talk can occur during signal recognition by the sensor kinase, as seen in metal sensing sensor kinases that can recognize non-cognate metals [76]. Secondly, it can result from phosphorylation of the response regulator by a non-cognate sensor kinase [77], and lastly, it can involve target gene transcription regulation by a non-cognate response regulator [78]. These cross-talks exponentially increase the complexity of the regulation cascades involving these systems, allowing for certain genes to be regulated by a histidine kinase sensor and not by its response regulator pair, and vice-versa [79].

Box 2

TCSs can be characterized according to their complexity. The most basic (Figure 6A) present a sensor kinase with one or more variable input domains, whose function is to detect stimuli, along with a conserved dimerization domain, where the highly conserved histidine that gets phosphorylated is present, and a conserved ATP binding domain with catalytic activity (Figure 6A). The response regulator presents a highly conserved receiver domain, which has the capability to both phosphorylate and dephosphorylate the response regulator, and a output domain [74]. More complex TCSs have conserved histidine phosphotransfer domains that act as intermediates in the phosphorelay, allowing for bidirectional phosphotransfer, that meaning phosphorylated His to Asp, as in the case of normal TCSs, but also from phosphorylated Asp to His (Fig 6B) [74]. TCSs have also been associated to the regulation of chemotaxis. In these cases, the sensor kinase domain presents changes in its structure, consisting in the replacement of the domain containing both the dimerization and His phosphorylation site by two independent domains, a His phosphotransfer domain and a domain dedicated to dimerization (Fig 6C). Since they participate in chemotaxis they do not present an input domain, relying instead on the CheW scaffold domain to receive the activation signal [80].

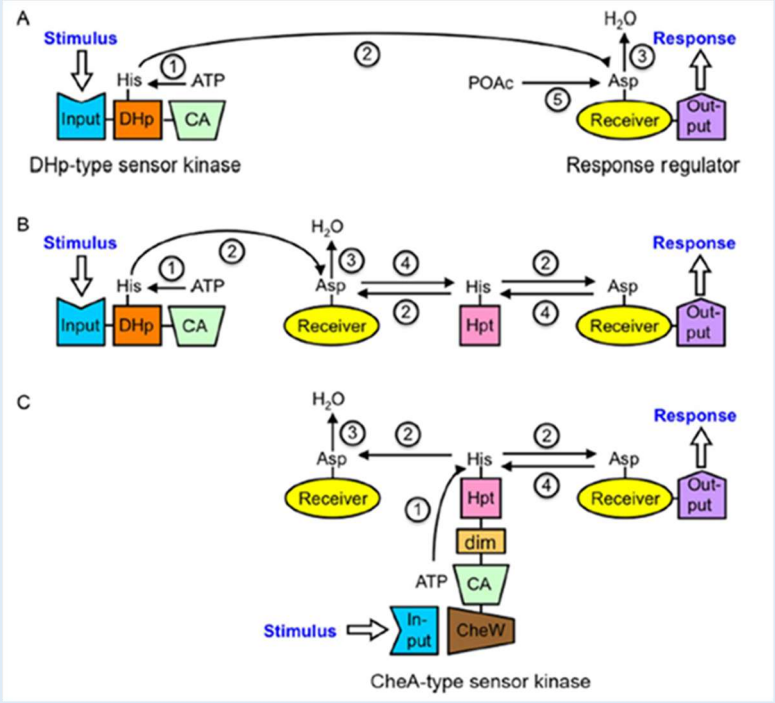

Figure 6 – Structure and phosphorelay mechanisms of TCSs. Schematic representation of a basic TCS **(A)**, a multistep phosphorelay TCS **(B)** and a chemotaxis TCS **(C)**. Reactions: (1) ATP-dependent sensor kinase autophosphorylation; (2) Phosphotransfer from histidine kinase to response regulator Asp; (3) Water mediated receiver domain autodephosphorylation; (4) Reverse phosphotransfer from receiver domain Asp to His from a histidine phosphotransfer domain (Hpt); (5) Alternative receiver domain phosphorylation, via small molecule phosphodonor, such as acetyl phosphate (POAc). Domains: Input (sensor domain); DHp (dimerization and histidine phosphorylation domain); CA (ATP binding catalytic domain); dim (dimerization domain); Chew (chemotaxis scaffold domain). Image adapted from [74].

Another layer of regulation involved in the control of TCSs are post-translational modifications (PTM), which include not only phosphorylation, but also acetylation and methylation [81-84]. It is known that N^{ε}-lysine acetylation alters protein conformation and/or charge. This results in changes in DNA-binding affinity, enzymatic activity, protein stability and protein-protein interactions [85]. Although this process is well known in

eukaryotes [86], not much was known about the regulatory process of acetylation in bacteria. Recent studies with PhoP, the response regulator of the PhoQP system of *Salmonella typhimurium*, have shed some light on this matter by demonstrating that the acetylation of residue K201, a key residue in DNA-binding [87], leads to a decrease in binding affinity, by disrupting the direct interactions between PhoP and its binding box [88]. This repression is important in early invasion stages, since PhoP inhibits the expression of the *Salmonella* pathogenicity island-1 (SPI-1) master regulator, HilA, that regulates transcription of bacterial invasion related genes [88, 89]. Upon the activation of the PhoPQ by environmental stimuli like Mg^{2+} and phagocytosis by macrophages, the levels of acetylation decrease, allowing for the activation of PhoP, which in turn upregulates the expression of *Salmonella* pathogenicity island-2 (SPI-2). This regulates the expression of the intra-macrophage exclusive T3SS Spi/Ssa and its secretome and is essential for survival in phagosomes [88, 90]. Another PTM that has been reported to regulate TCSs in bacteria is protein methylation. This modification is widespread in bacteria and has been shown to be necessary for virulence [82, 91, 92]. Methylation of arginine residues has been described to impair protein-protein interactions, by impairing the formation of salt bridges and hydrogen bonds that stabilize the dimer, thus inhibiting RR dimerization [84]. Glutamate and aspartate methylation impairs the formation of salt bridges and neutralizes the negative charge of the amino acid, thus preventing the binding of a phosphate group [82, 93]. This impairs phosphorylation of the sensor domain of RR, which is required for the activation cascade [82].

1.4 TCSs as potential drug targets

Since TCSs are present in all bacteria, with some playing major roles in cell growth and fitness [94, 95], while others regulate virulence factors or drug resistance [96-98], they present themselves as unique drug targets. Targeting these factors may allow impairing bacteria growth or diminishing their virulence and/or antibiotic resistance, culminating in cell death or reduced fitness [99]. Four main strategies for targeting TCSs have been developed, which include inhibition of sensor kinase activity, inhibition of response regulator activity, sequestration of signal and inhibition of signal generation [99].

Sensor kinases are a potential specific target for antibacterial therapy because bacteria utilize histidine sensor kinases, while mammals use serine/threonine kinases.

The first candidates for SK inhibitors, such as cyclohexenes, salicylanilides, trityls and benzoxazines, presented levels of inhibition ranging from 60% to complete inhibition of autokinase activity, although most of them presented low specificity and caused protein

aggregation, which is a non-specific mechanism of inhibition [100, 101]. These studies served as a basis for the development of other classes of inhibitors such as thienopyridine (TEP), that impaired sensor kinases from many bacteria, such as HpkA from *Thermotoga maritima*, VicK from *Streptococcus pneumoniae*, and EnvZ from *E. coli*, while not inhibiting mammalian kinases, and also not being toxic to rat myoblasts [102].

Response regulator activity requires two essential steps that can be targets for drug action: phosphorylation of a conserved aspartate residue and binding of the response regulator to DNA. Targeting the response regulator seems to present some advantage over sensor kinase inhibition, since the same response regulator can be phosphorylated by more than one sensor kinases via cross-talk [78, 103, 104] or by phosphate donor molecules like acetyl phosphate [74]. Lactoferricin B, a cationic antimicrobial peptide, has been shown to impair the phosphorylation of BasR and CreB from *E. coli* by impairing the binding of these RRs with their respective sensor kinases, thus impairing their phosphorylation [105]. Two alkyl imidazole derivatives have been described to impair binding between AlgR1 from *P. aeruginosa* and DNA, without interfering with the phosphorylation of AlgR1 or its cognate sensor kinase, AlgR2 [106].

The concept of signal sequestering, is based on impeding the activation of the sensor kinase, without altering the sensor domain [99]. AST-120, a drug that adsorbs indole, has been shown to affect indole-dependent signaling in *E.coli*, resulting in attenuated drug resistance and virulence [107]. It has been proposed that this effect is derived from the sequestering of indole, which activates CpxA and BaeS sensor kinases that induce the expression of antibiotic resistance-related genes, as well as the production of proteins from the type III secretion system [107-109].

DADMe-ImmucillinA compounds are transition state analogues of 5'-methylthioadenosine nucleosidase, which repress autoinducer-2 (AI-2) synthesis in *Vibrio cholerae* [110]. AI-2 plays a role in quorum-sensing and with its accessory receptor, dephosphorylate the LuxQ sensor kinase, resulting in the de-repression of ToxT [99, 110, 111]. ToxT will in turn upregulate the expression of virulence proteins such as cholera toxins [99]. By reducing the synthesis of AI-2, the DADMe-ImmucillinA compounds inhibit the generation of signal required for virulence in *V. cholerae* [99].

Although compounds that inhibit TCS activity seem promising, it is of note that these studies are still in their infancy. For example, the majority of the compounds identified have only been tested *in vitro* or *ex vivo*. Another problem is that these compounds present hydrophobic structures and low solubility. As such, in the future it will be necessary to conduct validation of the candidates in animal models of infection, as well as increase their hydrophilicity, to allow their use as antibacterial agents [99].

1.5 RstAB

The RstAB TCSs is a basic TCS from the OmpR/PhoB subfamily that was first described in *E. coli* [75], but has since then been identified in various bacteria, such as *Pseudomonas fluorescens* [112], *Clostridioides difficile* [113], *Salmonella* [104] and *Photobacterium damselae* subsp. *damselae* (*Phdd*) [94]. Its regulatory roles are bacteria-dependent and are often associated with stress-induced mechanisms. For example, RstAB from avian pathogenic *E. coli* (APEC) plays a key role in *hdeD*-mediated virulence leading to survival in chicken macrophages [114], whilst in *P. fluorescens* it has been associated with the expression of efflux pumps involved in multidrug resistance and with resistance to nitrosative stress [112]. In the case of *C. difficile,* the RstAB TCS was shown to regulate toxin production and sporulation, in a strain-dependent manner [115]. RstAB has also been shown to regulate virulence and modulate cell fitness in *Phdd*, as will be described in detail below.

The RstAB TCS is composed of a membrane embedded sensor kinase, RstB, and a response regulator RstA. RstB comprises a dimerization/His phosphotransfer domain, and a catalytic ATP binding domain, whilst RstA encompasses an aspartate phosphorylation site/dimerization site domain and a DNA binding domain, separated by a linker of variable size [116, 117].

In *E. coli*, under low Mg^{2+} and acidic pH (4.5), RstAB has been shown to be activated by the PhoQP TCS, although this has not been confirmed for RstAB from other bacteria [118]. It has also been demonstrated that once activated, the RstAB TCS can self-regulate its transcription, as demonstrated in *C. difficile,* in which it was shown that RstA binds to the *rstAB* promoter region and regulates its activity [113].

It has been proposed that the response regulator, RstA binds to a consensus sequence dubbed RstA box, comprised of TACATNTNGTTACA, with N being a variable base, and presenting two TACA recognition sites [118]. However, it has been reported that the classic RstA binding motif is absent in the promoter region of some genes regulated by RstA in *E.coli* and *Salmonella* [112, 119].

Like many other response regulators from the OmpR/PhoB subfamily, RstA forms a homodimer and this dimerization increases DNA binding affinity [120]. Salt-bridges are the key interactions in the formation of RstA-DNA complex, with a minor role associated to hydrogen bonds and van der Waals interactions [121, 122]. This was confirmed via crystal structure analysis of PhoP from *Mycobacterium tuberculosis*, a known RstA homologue [123] (Figure 7). With these analysis, it was determined that salt bridges

formed between residues R222, R223, K195 and R204 and the DNA coding strand are responsible for the primary interactions of PhoP with DNA, and that the binding affinity is mainly defined by the salt bridges formed between the side chains of R237 and both DNA strands [123] (Figure 7).

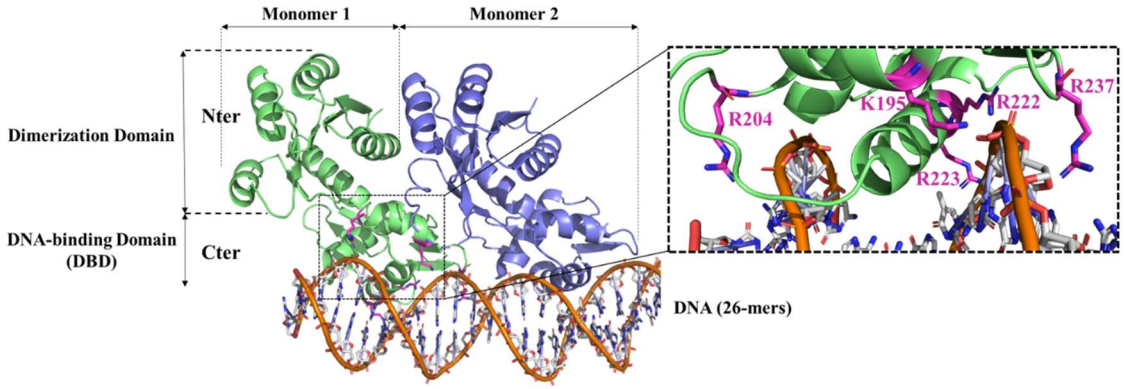

Figure 7 – Crystal structure of PhoP bound to DNA (pdb: 5ED4) with key residues involved in DNA interaction highlighted. *Left*: Three-dimensional structure of PhoP-DNA complex. The two PhoP monomers represented in cartoon (green and blue) bound to a DNA double strand (orange, 26-mers). *Right*: Close-up of the interaction of PhoP with DNA. Residues involved in the DNA binding are represented in magenta sticks (K195, R204, R222, R223 and R237).

These residues are highly conserved across members of the OmpR/PhoB subfamily, thus resulting in similar binding conformations in homologue proteins [123, 124]. Binding of DNA by RstA also relies on salt bridges. Indeed, isothermal titration calorimetry (ITC) showed that in RstA from *Klebsiella pneumoniae*, the mutation of residues R207 and R199, impedes binding of RstA to DNA suggesting that these residues are involved in RstA-DNA binding [116].

1.6 RstAB in *Photobacterium*

The RstAB in *Photobacterium* was first described in *Phdd*, when it was revealed that RstB positively regulates the expression of three hemolysins that play a major virulence role [96]. These are the plasmid-encoded damselysin (Dly), phobalysin P (PhlyP), and the chromosome-encoded phobalysin C (PhlyC). That work not only demonstrated that RstB was a major regulator of virulence in *Phdd*, but also showed its capability to regulate both plasmid- and chromosomal-encoded virulence genes [96]. Later, it was confirmed that RstA also regulated these same toxins, with both *rstA* and *rstB* mutants displaying impaired hemolytic activity [94]. Additionally, these *rstA* and *rstB* mutants have impaired motility, present deficiencies in cell growth and development, have reduced resistance to beta-lactams and are impaired in the production of proteins that require the T2SS for secretion, thus solidifying the role of RstAB as a major regulator of fitness and virulence in *Phdd* [94]. The latest study utilized RNA-sequencing to determine the genes regulated

by the RstAB system, revealing that besides the regulation of the previously mentioned toxins, it is also responsible for regulating the expression of outer membrane proteins, of genes associated with antimicrobial resistance and of new potential virulence factors [79] (Figure 8). One of the gene clusters that was found to be regulated by RstAB is involved in the production of a polysaccharide capsule that is important for resistance to the bactericidal action of fish serum and mucus and is required for virulence [79]. The work of Matanza and colleagues, demonstrated that although many genes identified by RNA-sequencing are regulated by both components of the RstAB system, some are regulated by just one component, thus providing evidence of regulatory cross-talks in *Phdd* [79].

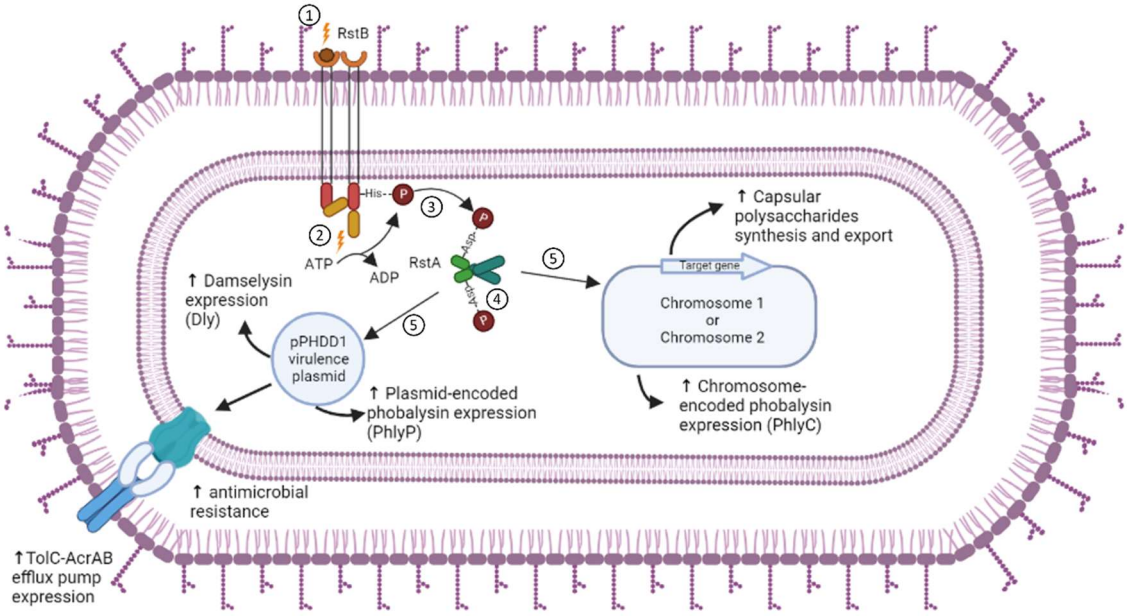

Figure 8 – RstAB regulates virulence and cell fitness in *Phdd*. Predicted mechanism of gene expression regulation by RstAB. Regulation mechanism occurs via a phosphorelay encompassing five steps: 1- Recognition of an environmental stimulus by RstB; 2- Autophosphorylation of a Histidine (His) in RstB; 3- Transfer of phosphate group to an Aspartate (Asp) residue in RstA; 4- Dimerization of RstA; 5- Regulation of gene expression by RstA. RstAB regulates expression of chromosome-encoded gene, such as hemolysins Dly and PhlyP and the TolC-AcrAB efflux pump and plasmid-encoded genes, such as hemolysins PhlyC, capsular polysaccharides synthesis and export related proteins. Image adapted from [80] and created with BioRender.com.

In *E. coli, Salmonella enterica* and in *Salmonella typhimurium*, RstAB gene expression has been described to be regulated by the PhoPQ TCS, in response to decreased concentrations of extracellular Mg^{2+} [104, 118, 125]. However, as for RstAB in *Phdd*, no activating stimuli have been identified so far, and no evidence for the regulation of RstAB by the PhoPQ TCS has been obtained.

To date, there are no reports of RstAB in *Phdp*, but unpublished data from FIV group revealed the existence of an operon containing the *rstA* and *rstB* genes in this bacterium (Figure 9).

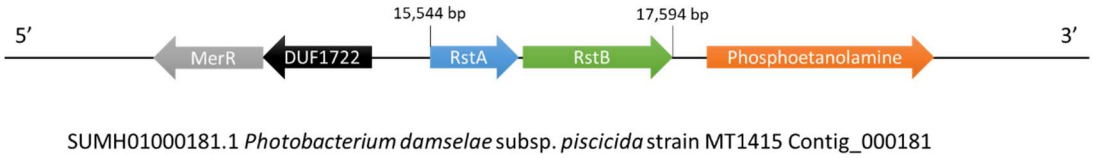

Figure 9 – Representation of the genomic context of the genes encoding RstAB in *Phdp*. RstA and RstB are encoded in an operon and share the same putative promoter region. Genes present in the contig 000181, (NCBI: SUMH01000181.1; RstA - WP_044180241.1; RstB - WP_044180240.1).

Phdp evolved from a subclade of *Phdd* and, as such, shares many similarities. However, during this evolution process, *Phdp* gained changes in the genome, due to loss and acquisition of genes [126]. Due to these changes, *Phdp* has developed host-specific virulence factors, as well as an infection mechanism that differs from the one of *Phdd* [126]. Despite these differences in virulence factors and pathogenicity mechanisms, it is likely that RstAB will also play a role in regulating *Phdp* virulence. This hypothesis stems from previous observations in *Phdd*, in which the deletion of RstAB TCS caused alterations not only the expression of virulence factors, but also in several aspects of cell fitness [94].

Aims:

Although the role of RstAB as a virulence regulator in *Phdd* has been described with some detail, the role of this TCS in the regulation *Phdp* virulence has not been investigated.

Unpublished data from the Fish Immunology and Vaccinology (FIV) group of i3S has uncovered the operon encoding this TCS in *Phdp*, and preliminary data obtained using a *rstB* deletion mutant revealed that this deletion resulted in decreased levels of AIP56 in ECPs, suggesting that RstAB regulates the expression of this important *Phdp* virulence factor. These observations set the basis for this work, aiming at clarifying the role of RstAB as a regulator of virulence in *Phdp*.

With this in mind, we aimed at:

1) Assessing the role of RstA and RstB in the regulation of expression of *Phdp* secreted proteins

2) Analyzing the interaction of RstA with the promoter regions RstB-regulated genes

3) Identifying the amino-acids residues of RstA involved in RstA-DNA interaction

2. Methods

2.1 Preparation of inocula for virulence assays

Bacterial stocks of *Phdp* MT1415 (WT), MT1415 Δ*rstB* (Δ*rstB*) and MT1415 Δ*rstB* complemented with plasmid-encoded *rstB* (Δ*rstB*+p*rstB*) were thawed and plated in Tryptic Soy Agar (TSA, Difco) with 1% NaCl (TSA-1) plates. In the case of the Δ*rstB*+p*rstB* strain, the TSA-1 medium was supplemented with chloramphenicol (Cam) at final concentration of 5 µg/mL. Plates were incubated at 25°C for 72 h. A swab was used to extract a sample of culture to a tube with Tryptic Soy Broth (TSB, Difco) with 1% NaCl (TSB-1). Bacterial suspensions were adjusted to an optical density at 600 nm (OD_{600}) of 0.5 and used to inoculate 100 mL TSB-1 at 1:100 dilution. Cultures were grown at 25°C until reaching OD_{600} of 0.9. Five mL of culture were collected and centrifuged at 3,220 g for 20 min at 4°C. The supernatant was discarded and the bacterial pellets were resuspended in TSB-1 to an OD_{600} of 0.7-0.8. These suspensions were diluted in TSB-1, to achieve the desired infection doses.

2.2 Fish maintenance and infection

Sea bass (*Dicentrarchus labrax*) were used for virulence assays. Fish were purchased from a commercial hatchery and maintained in 600 L seawater aquaria. Water temperature was maintained at 19 ± 2°C, salinity at 23–28‰, and the photoperiod was 14 h light: 10 h dark. Water quality was maintained with mechanical and biological filtration and ozone-disinfection and the fish were fed on commercial pellets (Skretting), adjusting the food intake to fish species/size and water temperature, according to the supplier's recommendations. All experimental protocols were carried out in accordance with European and Portuguese legislation for the use of animals for scientific purposes (Directive 2010/63/EU; Decreto-Lei 113/2013) and were licensed by the DGAV (Lic. 0421/000/000/2021). For infection, 25 fish per group (Experiment 1), with average weight of 33.6 ± 7.1 g or 23 fish per group (Experiment 2) with average weight of 89.9 ± 13.1 g were injected intraperitoneally with 100 µL of a bacterial suspension, obtained as described in section 2.1. In parallel, serial 10-fold dilutions of the inocula were plated in TSA-1 to quantify CFUs. Immediately after infection, the temperature was increased to 23 ± 1°C. Injected fish were monitored at least twice a day and mortalities recorded. Any fish showing signs of advanced disease (darkening of body color, lethargy, erratic swimming and loss of equilibrium) were euthanized, by immersion in 0.06% (*v*/*v*) of

ethylene glycol monophenyl ether followed by sectioning of the ventral aorta and counted as dead.

2.3 Bacterial growth curves

WT, Δ*rstB* and Δ*rstB*+p*rstB* strains were thawed and used to inoculate TSA-1 plates, as described in section 2.1. Bacteria were removed from the plates with a sterile swab and resuspended in TSB-1 to an OD_{600} of 0.5. This suspension was inoculated 1:100 in 4 mL of TSB-1. Aliquots (1 mL) of these inoculated media were transferred, in triplicate, to wells of a 24-well plate (Thermo Fisher Scientific). The remaining wells were filled with 1 mL of TSB-1 as negative control. The plate was sealed with a Breathe Easy membrane and OD_{600} were measured during 75 h at 1 h interval, using Sinergy 2 (Biotek Instruments) coupled to a Gen5 program (Biotek Instruments). The assay was carried out at 25°C with slow (continuous) shaking.

2.4 Production of MT1415 strains expressing PadA and PadB

To obtain MT1415 strains expressing PadA and PadB adhesins, MT1415Rif^R (rifampicin resistant) and MT1415Rif^{R}Δ*rstB Phdp* strains were transformed by conjugation with pMRB24 plasmids encoding PadA or PadB, respectively (Figure 10). Conjugation was performed using previously produced s17λpir *E. coli* strains complemented with pMRB24*padA* or pMRB24*padB* (s17λpir::pMRB24*padA* or s17λpir::pMRB24*padB,* respectively). For conjugation, a drop of filtered seawater was placed in a TSA-1 plate and used to suspend a colony of *Phdp* and a colony of donor *E. coli*. The drop was allowed to dry and the plates were incubated at 25°C for 24 h. A sample of the culture was then plated in a TSA-1 plate complemented with 50 µg/mL of Rif (to select *Phdp*) and 20 µg/mL of Cam (to select clones that incorporated the pMRB24 plasmid, which contains a gene encoding for Cam resistance). After 24 h of growth, colonies were screened by PCR using pMRB24-specific primers MRB24_F (CGCCTGCTATATGCTTGCAT) and MRB24_R (GCTGCTGGGATTACACATGG) [79] (Figure 10).

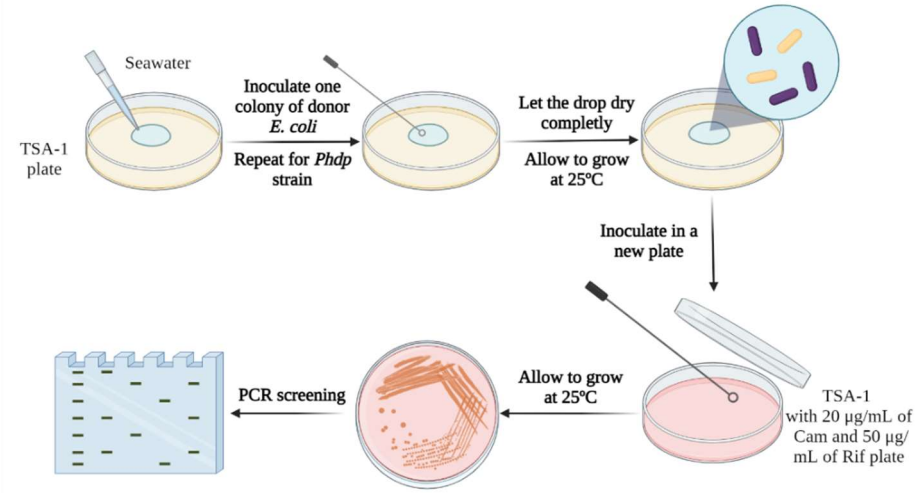

Figure 10 – Schematic representation of the protocol used for transformation of *Phdp* MT1415 with the pMRB24 plasmid encoding PadA or PadB. Image created with BioRender.com.

Positive clones (WT+p*padA*, WT+p*padB,* Δ*rstB*+p*padA* and Δ*rstB*+p*padB*) were inoculated in TSA-1 complemented with 20 µg/mL Cam and 50 µg/mL Rif and incubated at 25°C for 48 h. Bacterial mass was collected with a swab, suspended in 50% (v/v) of glycerol in TSB-1 and stored at -80°C.

2.5 Isolation of bacterial cells and ECPs

Bacterial stocks of WT, Δ*rstB*, Δ*rstB*+p*rstB,* WT+p*padA*, WT+p*padB,* Δ*rstB*+p*padA* and Δ*rstB*+p*padB* strains were defrost and plated in TSA-1, as described in section 2.1. A sample of each culture was collected and added to a tube with TSB-1 supplemented with appropriate antibiotics to achieve an OD_{600} of 0.5, were diluted 1:50 (v/v) in a final volume of 20 mL and were grown at 25°C for 24 h. After 24 h culture was diluted 1:5 in fresh medium to a final volume of 40 mL, in duplicate, and grown at 25°C until reaching OD_{600} of 0.4, 0.9 and 1.2. In the case of strains complemented with *padA* or *padB* (WT+p*padA*, WT+p*padB,* Δ*rstB*+p*padA* and Δ*rstB*+p*padB*), tubes were adjusted to an OD_{600} of 0.5, and were diluted in a ratio of 1:100 for a final volume of 40 mL in TSB-1 supplemented with chloramphenicol at final concentration of 5 µg/mL and were grown overnight (ON) at 25°C, until they reached OD_{600} of 0.9. Aliquots of 1.5 mL were removed from each culture and centrifuged 10 min at 10,000 g at 4°C. Pellets containing the bacterial cells were washed in 1 mL of TSB-1, centrifuged 10 min at 10,000 g at 4°C and stored at -20°C. Supernatants containing the ECPs were subjected to trichloroacetic acid (TCA) precipitation.

2.6 TCA precipitation

One ninth (v/v) of 100% (w/v) TCA was added to culture supernatants containing ECPs obtained as described in section 2.5. The resulting solution was vortexed and incubated for 30 min on ice followed by centrifugation for 15 min at 21,000 g at 4°C. The supernatant was discarded and the pellet was washed with TCA 10% (w/v), centrifuged for 15 min at 21,000 g at 4°C and washed with acetone, as just described. The acetone was discarded and the final pellet was air dried.

2.7 SDS-PAGE

Samples were dissolved in GLB 1x (50 mM Tris-HCl pH 8.8, 2% (w/v) SDS, 10% (v/v) glycerol, 0.017% (w/v) bromophenol blue, 2 mM ethylenediaminetetraacetic acid (EDTA) pH 8.8, 100 mM dithiothreitol (DTT)) and electrophoresed in a 14% polyacrylamide gel (Table 1).

Table 1 – Composition of 14% polyacrylamide gels used in SDS-PAGE

Running			Stacking		
Component	**Final concentration**	**Volume**	**Component**	**Final concentration**	**Volume**
30% acrilamide / 0.4% bis-acrilamide	14% (v/v)	7.04 mL	30% acrilamide / 0.4% bis-acrilamide	5% (v/v)	830 µL
1.875 M Tris pH 8.8	0.75 M	6 mL	0.6 M Tris pH 6.8	0.12 M	1.05 mL
10% SDS	0.1% (w/v)	150.4 µL	10% SDS	0.1% (w/v)	50 µL
TEMED	0.03% (v/v)	5.2 µL	TEMED	0.05% (v/v)	3 µL
10% APS	0.033% (v/v)	50.4 µL	10% APS	0.05% (v/v)	25 µL
Sterile water	-	1.76 mL	Sterile water	-	3.015 mL

Phdp cells and ECPs were run in gels with 140 mm width x 100 mm height x 1 mm thickness, for approximately 3 h at 40 mA, whereas *E. coli* fractions and aliquots from the protein purifications steps were run in mini-gels 86 mm width x 67 mm height x 1 mm thickness (Mini-PROTEAN BioRad) for 1 h at 200 V. Gels were stained with Coomassie Brilliant Blue R-250 (0.2% (w/v) Coomassie R-250, 50% (v/v) ethanol, 10% (v/v) acetic acid) for 30 min and destained with destaining solution (10% (v/v) ethanol, 10% (v/v) acetic acid).

2.8 Real Time-quantitative Polymerase Chain Reaction (RT-qPCR)

Bacterial stocks of WT and Δ*rstB* strains were thawed in TSA-1 and grown for 48 h at 25°C as described in section 2.1. Bacteria were removed from the plates with a sterile swab and resuspended in TSB-1 to an OD_{600} of 0.5. These suspensions were diluted 1:50 in TSB-1, to a final volume of 10 mL and incubated at 25°C for 24 h. Cultures were diluted 1:5 in TSB-1 to a final volume of 20 mL and grown at 25°C. When the OD_{600} reached 0.4 or 1.2, 10 mL of culture were collected and centrifuged at 4,000 g for 15 min at 4°C. Total RNA was isolated by the phenol-chloroform method described in [127], with some modifications. Briefly, after lysis, RNA was extracted using the TripleXtractor reagent (Grisp) and treated with DNase I (Turbo DNA-free, Ambion) following the manufacturer's recommendations. RNA purity and integrity was verified by 1% (w/v) agarose gel electrophoresis and Experion Automated Electrophoresis System (Bio-Rad Laboratories). One µg of RNA was reverse-transcribed into cDNA (iScript Kit, Bio-Rad Laboratories). Quantitative real-time PCR (qPCR) was performed in 20 µL reactions containing 1 µL of cDNA diluted 1:10 in dH_2O (or 5 µL of cDNA diluted 1:50 in the case of OMP19), 10 µL of SYBR Green Supermix (Bio-Rad Laboratories) and 0.25 µM of forward and reverse primers. The following cycling protocol was used: 1 cycle at 95°C (3 min) and 45 cycles at 95°C (20 s), 55°C (15 s) and 72°C (30 s). Data were normalized to the expression values of the housekeeping gene (16S rRNA) and analyzed by the comparative threshold (ΔΔCt) method [128].

2.9 Recombinant proteins

2.9.1 *In silico* analysis of RstA

The sequence of *Phdp* RstA was aligned with protein sequences of multiple RstA homologues obtained from UniprotKB (https://www.uniprot.org/) [129]. Sequence alignment was done using Clustal Omega multiple sequence alignment program (https://www.ebi.ac.uk/Tools/msa/clustalo/) [130].

An RstA model was generated, by homology modeling using the Phyre2 server [131]. Structures superposition was performed with PyMol program (The PyMOL Molecular Graphics System, Version 2.5.2, Schrödinger, LLC).

2.9.2 Site-directed mutagenesis of RstA

The different RstA mutants (R179A, R187A, R196A, K201A, R206A, K207A and R223A) were generated by site-directed mutagenesis, via inverse PCR, using a previously produced plasmid containing the full-length *rstA* cloned into the NcoI and XhoI restriction sites of pET28 in frame with a six His-tag at the C-terminus (pET28_RstA_FL) (Figure 11). To allow circularization of the plasmid using T4 ligase, the inverse PCR primers were phosphorylated using T4 polynucleotide kinase (T4 PNK) (Table 2).

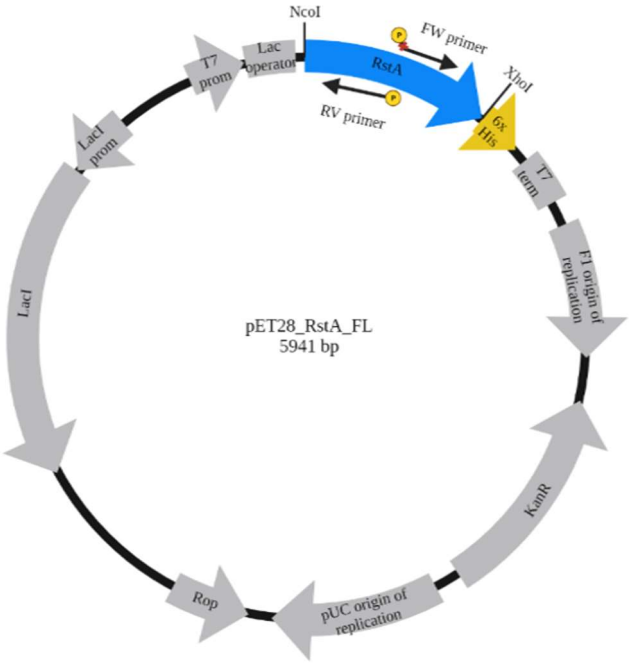

Figure 11 – Representation of the pET28_RstA_FL plasmid. Primers for inverse PCR present phosphorylated 5' ends (yellow ball). Mutation site is represented by the red cross. Due to the outward-pointing primers the entire sequence of the plasmid is amplified. The phosphorylated 5' end of the primers then allow the re-circularization of the plasmid containing the mutation via ligation. Image created with BioRender.com

Table 2 – Reaction for 5' phosphorylation of primers used in inverse PCR. Volumes were calculated in order to achieve a final concentration of 10 µM of phosphorylated primer in sterile water.

Reagent	Volume (µL)
100 µM oligo stock	2
10x T4 DNA ligase buffer	2
Sterile water	15
T4 Polynucleotide Kinase (T4 PNK)	1

The phosphorylation reaction was carried out at 37°C for 1 h, followed by inactivation of the T4 PNK at 65°C for 20 min, cooldown at room temperature (RT) and storage at -20°C.

Inverse PCR was conducted using the primers listed in Annex 1, using Q5 High-Fidelity DNA polymerase (New England BioLabs) and pET28_RstA_FL plasmid as template, with the conditions specified in Table 3.

Table 3 – Inverse PCR conditions

Step	Temperature (°C)	Time	Cycles
Initial denaturation	98	40 s	1
Denaturation	98	20 s	30x
Annealing	50	45 s	
Extension	72	4 min	
Final extension	72	5 min	1

The PCR products were analyzed by electrophoresis in a 1% agarose gel containing GreenSafe Premium (NZYTech) at 110 V for 30 min, in Tris-Acetate-EDTA (TAE) buffer (40 mM Tris + 1 mM EDTA + Acetic acid until pH 8.0). The whole volume of PCR product was loaded in 3 wells and the bands containing the recombinant plasmid were excised and purified using NZYGelpure kit, following the manufacturer's instructions, with a final elution in 30 µL of elution buffer.

The purified plasmid containing the mutation was quantified using NanoDrop One (Thermo Fisher Scientific) and re-circularized, using T4 ligase (Thermo Fisher Scientific) at a final concentration of 5 U/µL and 100 ng of plasmid in a final volume of 15 µL. Ligation was performed at 4°C ON in order to conduct bacterial transformation.

2.9.3 Bacterial transformation

For plasmid amplification, bacterial transformation was conducted using chemically competent *E. coli* DH5α, produced via calcium chloride method [132]. For protein expression, bacterial transformation was conducted using chemically competent *E. coli* BL21 (DE3) cells. Transformation was conducted via heat shock [133]. Briefly, 100 µL of competent cells were incubated with 100 ng of plasmid for 30 min on ice, or the whole volume of the ligation for 5 h on ice and subjected to a heat-shock by heating the cells for 45 s at 42°C followed by an incubation for 5 min on ice to reestablish the membrane potential. Afterwards, cells were inoculated in 900 µL Luria-Bertani broth (LB) and grown

for 1 h at 37°C (200 rpm). For obtaining starter cultures for plasmid amplification, cultures were centrifuged at 4,000 g for 5 min at RT. After removing 800 µL of supernatant the bacterial pellet was resuspended in the remaining medium, plated on LB agar with 50 µg/mL of kanamycin (Kan) and incubated at 37°C ON. For protein expression, the 900 µL of culture were inoculated in 10 mL of LB with 50 µg/mL Kan and grown ON at 37°C (200 rpm).

2.9.4 Plasmid purification

Isolated colonies from ON cultures in LB agar were screened by PCR to confirm if the colonies were positive for the gene of interest. Two positive colonies were inoculated in 10 mL of LB with 50 µg/mL Kan and grown ON at 37°C (200 rpm). Bacterial cultures were centrifuged at 4,000 g for 20 min at 4°C. Supernatant was discarded and the pellet was used for plasmid extraction using the NZYMiniprep kit, following the manufacturer's instructions, with a final elution in 40 µL of elution buffer.

2.9.5 Protein expression

E.coli BL21 (DE3) cells transformed with plasmid encoding the protein of interest were grown ON at 37°C in 10 mL LB supplemented with 50 µg/mL Kan. This ON culture was used to inoculate 1 L of LB supplemented with Kan at the same concentration. Cultures were grown at 37°C until reaching an OD_{600} of 0.4-0.6. Protein expression was induced by adding Isopropyl β-D-1-thiogalactopyranoside (IPTG) to a final concentration of 0.5 mM. Following 4 h incubation at 37°C (200 rpm), cultures were centrifuged using High Speed Centrifuge Beckman Avanti J-26 XP at 3,057 g for 30 min at 4°C. The supernatants were discarded and the pellets resuspended in 40 mL of 50 mM HEPES pH 7.0, 300 mM NaCl, 25 % (v/v) glycerol, 1 mM DTT, and frozen at -20°C.

2.9.6 Affinity chromatography

The suspensions of induced bacterial cells were thawed on ice, sonicated with a Sonifier 250 (Branson) (duty cycle – 70%; output control – 40; 2 x 30 s) and centrifuged at 35,000 g, 4°C, for 30 min, to separate the soluble and insoluble fractions.

Proteins were purified from the soluble fractions by Immobilized Metal Ion Affinity Chromatography (IMAC) using a gravity flow chromatography column with nickel resin (ABT). Recombinant proteins with His-tag bind to nickel ions present in the resin, allowing for the separation of the tagged from the remaining proteins. Following a wash

step with 50 mM HEPES pH 7.0, 300 mM NaCl, 25% (v/v) glycerol, 1 mM DTT, 20 mM imidazole, elution of RstA was achieved with 50 mM HEPES pH 7.0, 300 mM NaCl, 25% (v/v) glycerol, 1 mM DTT, with increasing concentrations of imidazole (100 mM, 200 mM, and 400 mM). A 10 mL fraction was collected at each elution step. Five µL of the soluble and insoluble fractions and 10 µL of the flow through and elutions were analyzed by SDS-PAGE and fractions containing the best ratio of protein/contaminants were selected and pooled for dialysis.

2.9.7 Dialysis and concentration

Following IMAC, protein samples were dialyzed ON at 4°C against 200 volumes of 50 mM HEPES pH 7.0, 300 mM NaCl, 25% (v/v) glycerol, 1 mM DTT, using a membrane with a cut-off of 6-8 kDa (Spectrum Labs), to reduce the concentration of imidazole.
After dialysis, the proteins were removed from the membrane and centrifuged to eliminate precipitated protein. If deemed necessary, protein samples were concentrated at 4°C using centrifugal concentrators with a cut-off of 10 kDa (Vivaspin 20, Sartorius). Proteins were then aliquoted and stored at -80°C.

2.9.8 Analysis of protein concentration and purity

Protein concentration was determined using NanoDrop One (Thermo Fisher Scientific), using the expected molecular weight and the molar extinction coefficient calculated by the ProtParam tool (https://web.expasy.org/protparam/) [134]. Coomassie blue-stained gels were scanned using GS-900 Calibrated Densitometer (Bio-Rad) and protein purity was analyzed by densitometry using the Image Lab software (Bio-Rad).

2.9.9 Thermal shift assay

Thermal shift assay (also called differential scanning fluorimetry (DSF) or ThermoFluor) (Figure 12) was conducted to improved buffer conditions for RstA recombinant proteins. Two homemade 96 well plates (Annex 2) were prepared: one (Plate A) contained solutions with increasing concentrations of salt (0-1000 mM) and varying buffers in a range of pHs (4.5-10); the other (Plate B) contained various ligands and increasing concentrations of glycerol (0-50%). Each well contained 12.5 µL of solution.
Proteins were diluted in buffer (50 mM Tris pH 8.0, 300 mM NaCl) to a final concentration of 1 mg/mL and each well previously filled with 12.5 µL of buffer was loaded with 7.5 µL of protein. The plate was sealed with a transparent sealing membrane (BioRad),

centrifuged at 201 g for 1 min, and incubate for 30 min at RT. Five µL of a 25x stock solution of SYPRO Orange were added to each well, to achieve a 5x final concentration. The plate was sealed with a new film, centrifuged for 1 min at 201 g and analyzed in a Real-Time PCR (CFX96 Touch Deep Well Real-Time PCR System (Bio-Rad)), with the following program: Melt Curve analysis, starting at 25°C with increments of 0.5°C every 30 s, until 95°C.

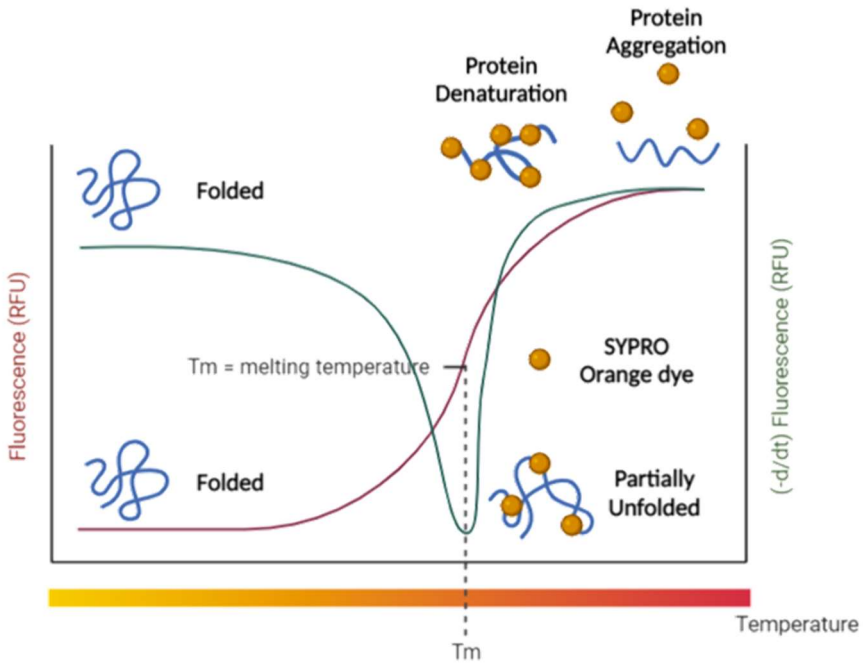

Figure 12 – Thermal shift assay. In the thermal shift assay, a protein is exposed to increasing temperatures in the presence of SYPRO Orange that has an affinity to hydrophobic regions. With the increase in temperature, protein will unfold and expose hydrophobic regions. SYPRO Orange will bind to the hydrophobic regions, leading to an increase in fluorescence. Melting temperature (Tm), can be determined at the point when half the protein is unfolded. This point is more easily identified by the peak obtained by the negative derivative of fluorescence across time (-d(RFU)/dT). Image created with BioRender.com

2.9.10 Circular dichroism

RstA and mutant RstA proteins were thawed and dialyzed ON at 4°C against 2000 volumes of 20 mM HEPES pH 7.0, 300 mM NaF, 10% (v/v) glycerol, 1 mM DTT, using a membrane with a cut-off of 6-8 kDa (Spectrum Labs). After dialysis, the proteins were removed from the membrane and centrifuged to eliminate precipitated protein. Supernatant was collected and protein concentration was determined by NanoDrop One (Thermo Fisher Scientific). Proteins were diluted in 500 mM NaF at a final concentration of 100 µg/mL in a volume of 250 µL and loaded in a 1 mm x 10 mm quartz cuvette. Circular dichroism was conducted using J-815 CD Spectometer (Jasco) and Spectra Manager software (Jasco), with 8 accumulations per sample, scan speed of 20 nm/min and a scan range from 260 to 190 nm.

2.10 Electrophoretic Mobility Shift Assay (EMSA)

2.10.1 Amplification of putative promoter regions

Putative promoter regions were amplified by PCR, using genomic DNA from *Phdp* strain MT1415 as template, with the primers described in Annex 3. PCR reactions were performed using NZYTaq II 2x Green Master mix polymerase (NZYTech) (30 s/kb). Each reaction contained 100 ng of template DNA and 0.5 µM of each primer, and PCR was conducted in the conditions specified in Table 4.

Table 4 – PCR conditions for production of putative promoter regions used in EMSA

Step	Temperature (°C)	Time	Cycles
Initial denaturation	95	3 min	1
Denaturation	95	45 s	30x
Annealing	50	45 s	
Extension	72	15 s	
Final extension	72	10 min	1

PCR products were run in a 1% agarose gel at 110V for approximately 30 min in TAE (section 2.9.2), using GeneRuler 1kb DNA Ladder (Thermo Fisher Scientific) as size marker. Amplicons with the right size were excised from the gel with a scalpel and purified using NZYGelPure kit following the manufacturer's instructions. DNA concentration was determined using NanoDrop One (Thermo Fisher Scientific). Putative promoter regions and corresponding size are described in Table 5.

Table 5 – Sizes of the putative promoter regions used in EMSA

Promoter	Size (bp)
aip56	373
pbt	353
pla	231
pnpA	480
omp19	250
padA	574
padB	247

2.10.2 Native gel preparation

EMSAs were conducted using 5% acrylamide/bis-acrylamide native gels (Table 6) with 100 mm width x 8.3 mm height x 1 mm thickness, using the MiniProtean Tetra (BioRad) system. The gels were left to polymerize for 2 h at RT and were stored at 4°C ON prior to use.

Table 6 – Composition of EMSA gels

Component	Volume
10x TAE	1.0 mL
40% acrylamide/bis-acrylamide (75:1)	1.25 mL
Sterile water	7.75 mL
10% APS	60 µL
TEMED	6 µL

2.10.3 DNA-protein binding

Samples used in EMSAs contained 2 nM of promotor DNA (plus 20 nM of competitor DNA in the case of competition EMSAs) and increased concentrations of protein (0, 50, 100 and 200 nM) in binding buffer (50 mM Tris-HCl pH 7.5, 0.5 mM EDTA, 50 mM KCl, 10 mM $MgCl_2$, 3 µM bovine serum albumin (BSA), 10% (v/v) glycerol, 1 mM DTT, 10 mM acetyl phosphate), in a final volume of 10 µL. Binding reaction was conducted for 30 min at RT, during which the gels were pre-ran at 80V.

2.10.4 EMSA

In this technique, DNA samples incubated or not with protein are loaded into a native polyacrylamide gel. A well is loaded with free DNA in order to set the benchmark of migration for that specific DNA. This is then used as a comparison with lanes loaded with DNA incubated with protein. If protein binds to DNA, the complex formed will have a higher molecular weight than free DNA and, as such, will migrate slower, resulting in a "shift" upwards of the DNA band. On the contrary, if no binding occurs, DNA will migrate as free DNA (Figure 13).

All EMSAs were run in a 4 ºC cold chamber at 10 $V.cm^{-1}$, using EMSA TAE (40 mM Tris-HCl pH 7.8, 2.5 mM EDTA) as running buffer. Upon loading of the samples, the gel was run at 200 V for 5 min in order to stack the samples and guarantee that they enter the

gel. Afterwards, the gel was run at 80 V for 40 min (or 1 h in competition EMSAs). Gels were stained for 15-20 min with GreenSafe Premium (NZYTech) in EMSA TAE (1:50 v/v), whilst covered from the light, and were visualized in a BioRad Gel Doc EQ system, using the software Image Lab (BioRad).

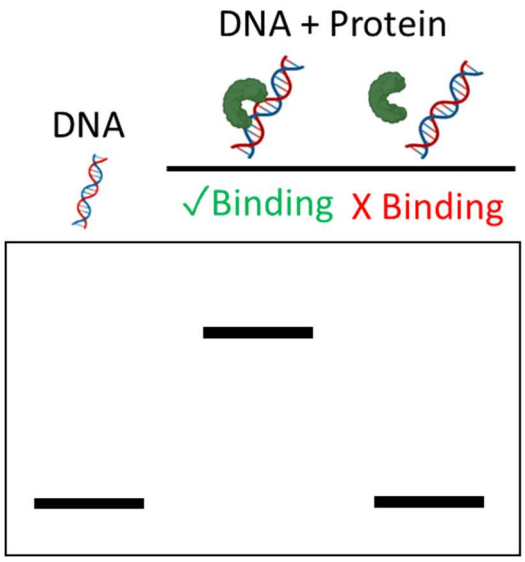

Figure 13 – Schematics of EMSA. DNA or DNA incubated with protein are loaded into a native polyacrylamide gel. Free DNA sets the benchmark of migration. If protein binds to DNA, the complex will migrate slower and a "shift" will be observed, whereas if no binding occurs DNA will migrate as free DNA.

3. Results

3.1 RstB regulates *Phdp* virulence

3.1.1 Deletion of *rstB* in MT1415 results in impaired virulence for sea bass

RstAB has been shown to be a master regulator of virulence in *Phdd* [94]. Although *Phdp* harbors an rstAB operon (Figure 9), nothing is known about its role in regulating virulence in this subspecies. To investigate if RstAB is involved in the regulation of *Phdp* virulence, we conducted virulence assays in sea bass using a wild-type MT1415 strain (WT), a MT1415 *rstB* knockout strain (Δ*rstB*), and a MT1415 knockout strain complemented with plasmid-encoded *rstB* (Δ*rstB*+p*rstB*). We could not assess the role of RstA because despite several attempts, it was not possible to obtain a *rstA* deletion mutant in *Phdp*. Prior to the virulence assays, we confirmed that Δ*rstB* and Δ*rstB*+p*rstB* strains grew similar to the WT (Figure 14).

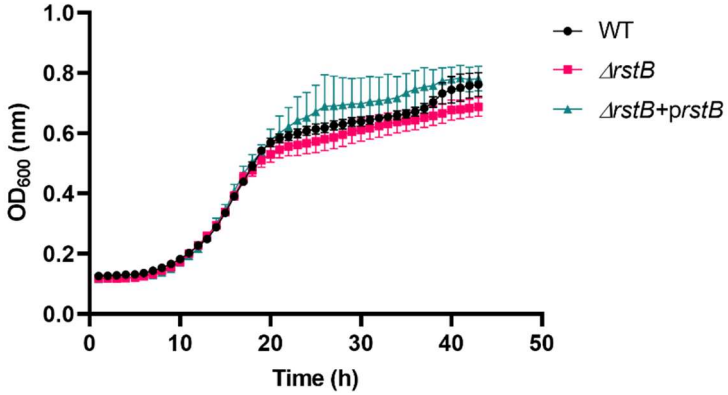

Figure 14 – Growth curves of WT, *ΔrstB* and *ΔrstB*+p*rstB* strains. Strains of *Phdp*, WT, Δ*rstB* and Δ*rstB*+p*rstB* were grown in TSB-1 at 25°C, with slow shaking in wells of a 24-well plate. OD at 600 nm (OD_{600}) were measured at 1 h interval during 75 h. Values in the graph correspond to the mean±SD of OD_{600} from triplicate wells. Results shown are representative of three independent experiments.

Following growth analysis, we conducted two independent virulence assays (Figure 15). In experiment 1, performed with fish with an average weight of 33.6 ± 7.1 g, the WT strain induced 79% mortality, whereas no mortality was observed after injection of the *rstB* knockout strain (Δ*rstB*). As expected, complementation with plasmid-encoded *rstB* (Δ*rstB*+p*rstB*) resulted in a mortality similar to the one obtained with the WT strain (84%).

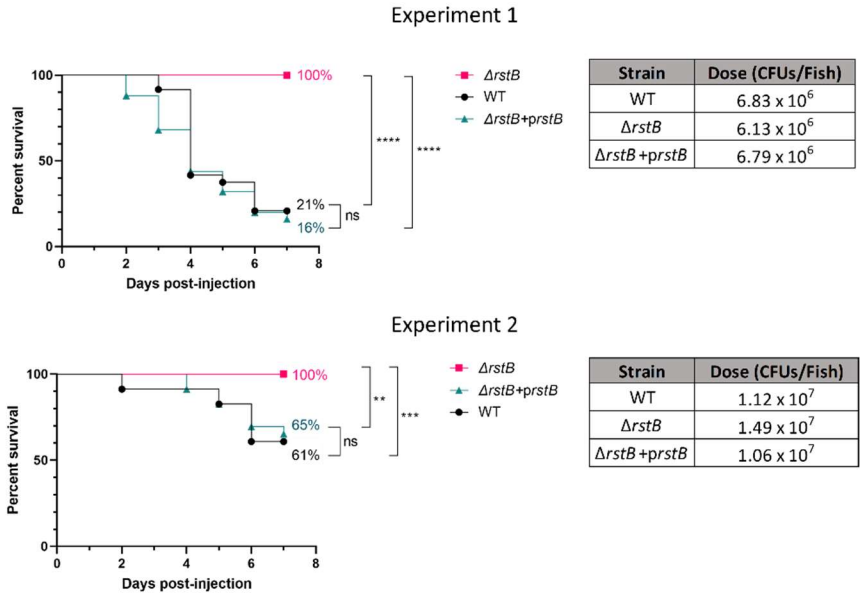

Figure 15 – Deletion of *rstB* abolishes *Phdp* virulence for sea bass. Kaplan-Meier survival curves of sea bass injected i.p. with the indicated strains. Experiment 1 – average weight of 33.6 ± 7.1 g, n=25 fish per group. Experiment 2 - average weight of 89.9 ± 13.1 g, n=23 fish per group). Curve comparisons were performed using the log-rank test (95% confidence). Asterisks represent statistical difference: ***p*<0.01, ****p*<0.001, *****p*<0.0001, ns no statistical difference.

In experiment 2, using bigger fish (89.9 ± 13.1 g), the WT strain induced 35% mortality, and again, no mortality was observed after injection with the Δ*rstB* strain. The mortality

in the group infected with the Δ*rstB+prstB* strain (39%) was similar to the mortality induced by the WT. These results clearly show that *rstB* is required for *Phdp* virulence.

3.1.2 RstB controls expression of virulence factors in *Phdp* MT1415

Next, we aimed at understanding the mechanism by which RstB influences *Phdp* virulence. It is known that *Phdp* virulence is highly dependent on secreted factors [11]. Amongst them is the apoptosis-inducing protein AIP56 [6] and PBT, a binary toxin composed of PBTa and PBTb that is highly toxic to macrophages (Unpublished data from FIV Group). With this in mind, we compared the protein profiles of cells and culture supernatants from the WT, Δ*rstB* and *ΔrstB*+p*rstB* strains, obtained in three stages of cell growth (Figure 16).

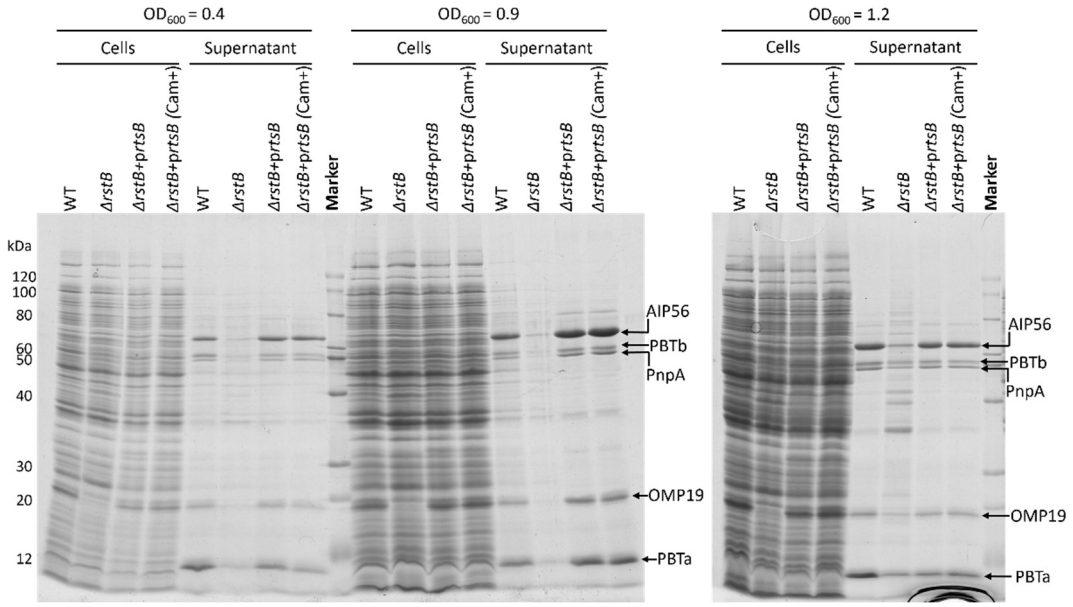

Figure 16 – Deletion of *rstB* results in decreased levels of AIP56, PBTa, PBTb, PnpA and OMP19 in the *Phdp* culture supernatants. SDS-PAGE of bacterial cells and culture supernatants from WT, Δ*rstB* and *ΔrstB*+p*rstB* strains grown in TSB-1 until early exponential (OD_{600} = 0.4), late exponential (OD_{600} = 0.9) and stationary (OD_{600} = 1.2) phases. In the case of the *ΔrstB*+p*rstB* strain, which harbors a plasmid conferring chloramphenicol (Cam) resistance, cultures were also performed in TSB-1 with 5 µg/mL chloramphenicol (Cam+). After electrophoresis, the gel was stained with Coomassie-blue. Marker: GRS unstained protein ladder (GRiSP). Numbers at the left indicate the molecular weight of the markers, in kDa.

The protein profiles obtained by SDS-PAGE showed that deletion of *rstB* leads to a strong decrease in the amount of AIP56 and PBT (PBTa and PBTb) in the supernatants. Since both toxins cause death of macrophages and have a crucial role for virulence in sea bass ([6] and Unpublished data from FIV Group), their reduced expression likely explains the attenuated virulence of the Δ*rstB* strain. SDS-PAGE also revealed that *rstB* deletion resulted in decreased levels of the peptidoglycan hydrolase PnpA [17], as well

as of OMP19, a newly identified and very abundant outer membrane protein (Unpublished data from FIV Group).

To determine whether the decreased amounts of AIP56, PBT and PnpA in the supernatants of the Δ*rstB* strain correlate with a diminished transcription of the corresponding genes, a RT-qPCR analysis was performed (Figure 17).

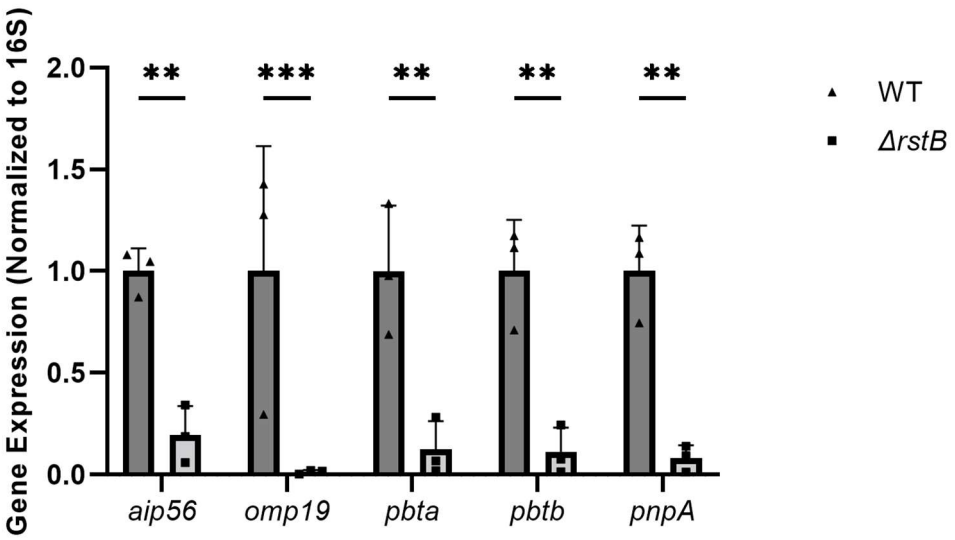

Figure 17 – Deletion of *rstB* leads to decreased expression of *aip56*, *omp19, pbta, pbtb* and *pnpA.* Expression levels of the indicated genes in the WT and Δ*rstB* strains grown TSB-1 until late exponential (OD_{600}=0.9) were determined by RT-qPCR. Conditions of RNA isolation and synthesis of corresponding cDNA, as well as RT-qPCR protocol are described in section 2.8. Gene expression was normalized to expression of housekeeping gene 16S. Data represent the means ± SD of three independent experiments. Measurements of each experiment were made in duplicate. Statistical analysis was performed using Two way-Anova (**p<0.01, ***p<0.001).

In agreement with the SDS-PAGE results, RT-qPCR show that deletion of *rstB* leads to a decrease in expression of *aip56*, *pbta*, *pbtb*, *pnpA*, and *omp19*. This indicates that RstB positively regulates the expression of *aip56, pbta, pbtb, pnpA* and *omp19* genes.

3.1.3 RstB regulates expression of PadA

To determine if expression of the recently identified PadA and PadB adhesins is regulated by the RstAB TCS, we transformed WT and Δ*rstB* MT1415 strains, which lack the PadA and PadB encoding genes, with a plasmid encoding each of these adhesins under the control of their respective endogenous promoter and analyzed their expression by SDS-PAGE (Figure 18).

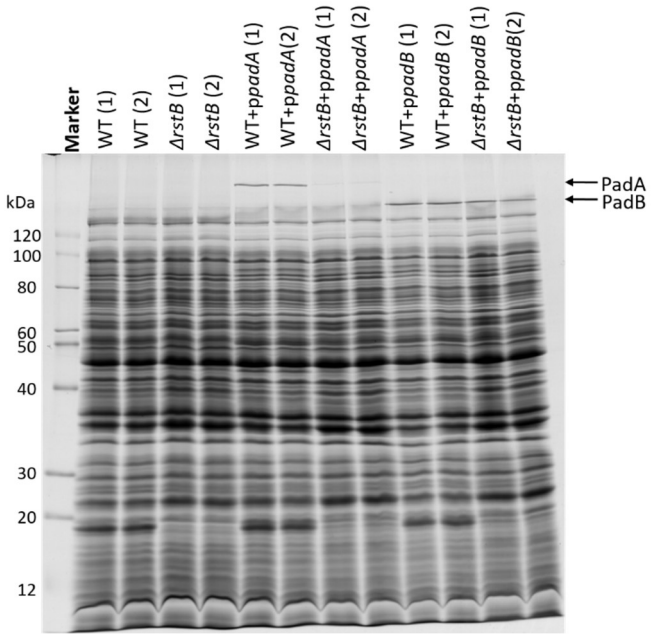

Figure 18 – Analysis of PadA and PadB expression in WT and Δ*rstB* MT1415 strains. SDS-PAGE of bacterial cells of MT1415 (WT) and MT1415 Δ*rstB* (Δ*rstB*) *Phdp* strains complemented with either PadA or PadB. As seen deletion of *rstB* leads to a decrease in the expression of PadA, while no differences can be seen for PadB. This suggests that PadA is regulated by the RstAB TCS. Marker: GRS unstained protein ladder (Grisp). Numbers at the left refer to the molecular weight of the markers, in kDa, and numbers between brackets refer to two independent cultures.

As expected, PadA and PadB were not detected in the WT and Δ*rstB* cells. However, after transformation of these strains with a plasmid encoding PadA (p*padA*), this protein was detected in the lanes loaded with WT+p*padA* cells but not in the lanes corresponding to the Δ*rstB*+p*padA*. This indicates that RstB is required for expression of PadA. In contrast, expression of PadB is not dependent on RstB, because the amounts of PadB in the WT+p*padB* and Δ*rstB*+p*padB* cells are similar (Figure 18). Altogether, these results suggest that RstB regulates the expression of *padA*, but not *padB*.

3.2 RstA interacts with the promoter regions of *aip56, pbt, pnpA, omp19, padA* and *padB*

Although many of the genes regulated by RstB are also regulated by its cognate pair RstA [79], mechanisms of cross-talk between RstA and RstB with other TCSs have been described [76, 78, 79]. Thus, we decided to investigate if the genes regulated by RstB are also regulated by RstA, i.e., if regulation by RstB occurs via the canonical RstAB pathway. For this, we asked if RstA interacts with the promoter regions of the secreted factors shown to be regulated by RstB in section 3.1.2 and section 3.1.3.

3.2.1 Optimization of RstA production

In a previous work (developed under the scope of my Bachelor degree internship at FIV group), we had already obtained recombinant RstA protein. However, the protocol used for obtaining this protein had low yield and produced a protein with low stability and many contaminants (Figure 19), unsuitable for molecular studies. Therefore, in this work, we started by optimizing the production and purification of recombinant RstA.

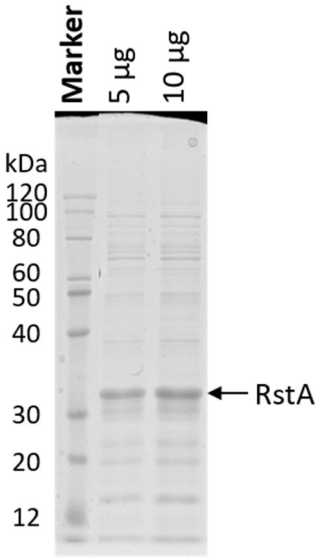

Figure 19 – Recombinant RstA available at the beginning of this work. Coomassie blue-stained SDS-PAGE gel of the previously produced RstA recombinant protein (29.2 kDa). Gel was loaded with 5 and 10 µg of protein. Note that the preparation contained many contaminants. Numbers at the left refer to the molecular weight of the markers, in kDa. Marker: GRS unstained protein ladder (GRiSP).

The first step was to select a buffer favoring RstA stability. For this, we performed a Thermal shift assay, which allows to determine the stability of a protein under varying conditions by measuring changes in the thermal denaturation temperature (Figure 20). In this assay, the denaturation midpoint of a protein is defined as the melting temperature (Tm) in which there is an equilibrium between its folded and unfolded states. As such, a higher Tm (temperature required to achieve 50% denaturation of the protein population) indicates a more stable protein.

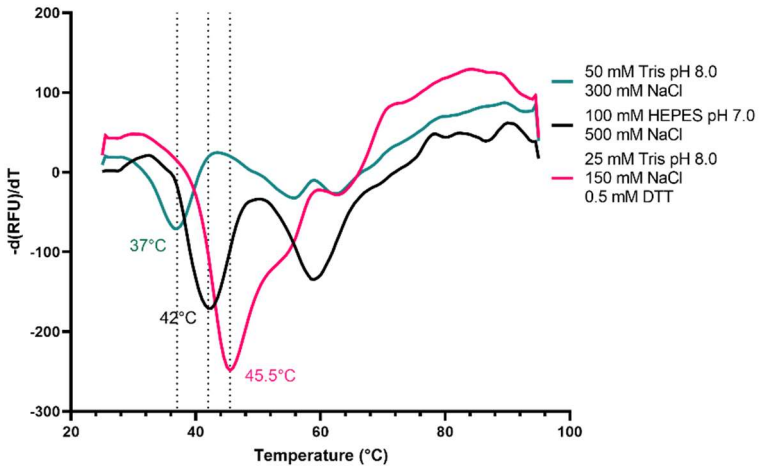

Figure 20 – Thermal shift assay of RstA. RstA was incubated in buffers with increasing salt concentrations and different pH values in the presence of SYPRO Orange dye. RstA in the nitial buffer (green) presented a Tm = 37°C, whereas the protein in a HEPES based buffer (black) presented a Tm = 42°C. RstA in the the initial buffer supplemented with 0.5 mM final concentration of DTT displayed a Tm = 45.5°C (pink).

Thermal shift analysis showed that RstA in the previously used buffer containing 50 mM Tris pH 8.0, 300 mM NaCl (Figure 18, green line) presented a Tm of 37°C. Changing the buffer to 100 mM HEPES pH 7.0, 500 mM NaCl increased Tm to 42°C (black line) and addition of 0.5 mM of DTT resulted in a Tm of 45.5°C (pink line). Based on these results, we produced a new batch of recombinant RstA using a buffer containing 50 mM HEPES pH 7.0, 300 mM NaCl, 25% (v/v) glycerol, 1 mM DTT.

Chemically competent *E. coli* BL21(DE3) were transformed with pET28_RstA_FL, protein expression was induced with 0.5 mM IPTG at 37°C for 4 h, and RstA was purified from the soluble fraction of induced *E. coli* cells by IMAC. Fractions were collected during purification to evaluate protein yield and solubility (Figure 21A). Elutions containing the best ratios of RstA/contaminants were pooled, dialyzed, and concentrated.

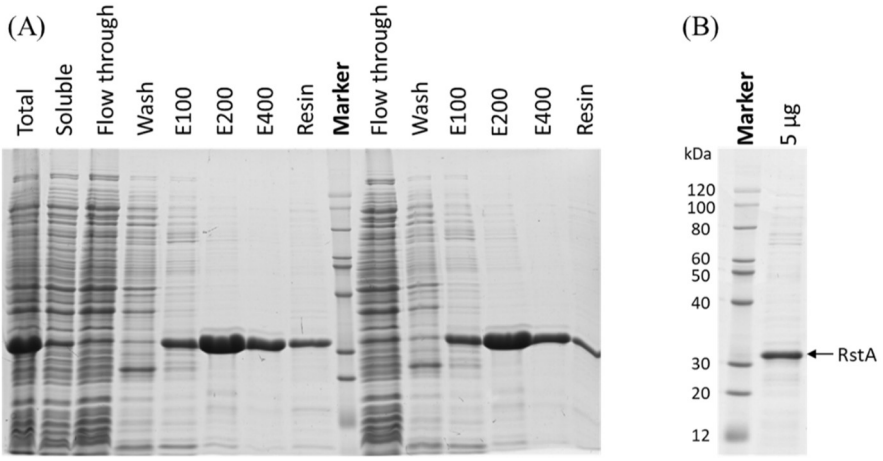

Figure 21 – Production and purification of RstA. (A) SDS-PAGE analysis of the fractions collected during purification of RstA by IMAC. RstA was eluted with 50 mM HEPES pH 7.0, 300 mM NaCl, 25% (v/v) glycerol, 1 mM DTT, containing 100, 200 and 400 mM of imidazole (E100, E200 and E400, respectively). Fractions E200 and E400 were selected, pooled

and dialyzed ON to remove imidazole. After dialysis, protein was concentrated via ultrafiltration. **(B)** SDS-PAGE analysis of RstA obtained after purification, dialysis and concentration. Gel was loaded with 5 µg of protein. The optimized buffer allowed to obtain an RstA batch at a concentration of 1.3 mg/mL and with 85% purity. Numbers at the left in panel (B) refer to the molecular weight of the markers, in kDa. Marker: GRS unstained protein ladder (GRiSP).

This optimized purification protocol resulted in improved yields and allowed to obtain a purer and more stable protein preparation (Figure 21B).

3.2.2 Phosphorylation of RstA leads to its dimerization

It is known that many response regulators need to be phosphorylated, in order to dimerize and bind to DNA [75, 135]. This phosphorylation occurs in a highly conserved aspartate residue and requires four highly conserved residues in the vicinity [74, 136]. These residues are two negatively charged glutamate or aspartate residues that coordinate a divalent cation (usually Mg^{2+}), a positively charged lysine, and either a threonine or a serine residue [136]. This phosphorylation site has been studied in the RstA homologue AdeR, and was shown to comprise an aspartate residue phosphorylated (D63), two negatively charged residues that coordinate Mg^{2+} (E19 and D20), a positively charged lysine (K104), a threonine (T82) and a lysine (K65) that participates in coordination of Mg^{2+} [124] (Figure 22).

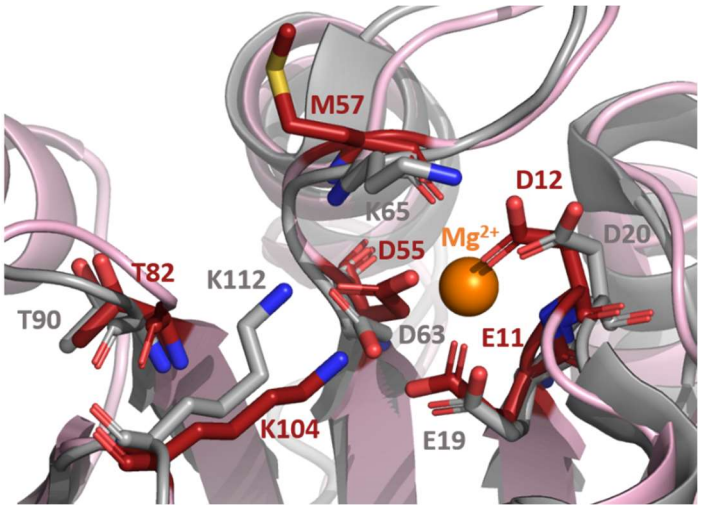

Figure 22 – *In silico* prediction of the RstA phosphorylation site. Superposition of AdeR receiver domain coordinated with Mg^{2+} (gray, PDB: 5XJP) and RstA model (light pink) generated by Phyre2 [131]. The residues involved in the phosphorylation of AdeR and the corresponding residues in *Phdp* RstA are represented in gray and dark red sticks, respectively. Mg^{2+} represented as orange sphere. It is of note that RstA presents a methionine residue (M57), in place of a lysine that in AdeR (K65) coordinates binding with Mg^{2+}. Obtained using Pymol program.

Since these five residues are conserved in RstA (Figure 22, red sticks), we aimed at investigating if phosphorylation is required for RstA dimerization. It is of note that RstA presents a methionine (M57), whereas in AdeR the corresponding residue is a lysine (K65) [124]. Firstly, we conducted a size exclusion chromatography using RstA in the absence or presence of 10 mM of acetylphosphate, a compound shown to act as a phosphodonor in bacterial cells [137, 138] (Figure 23).

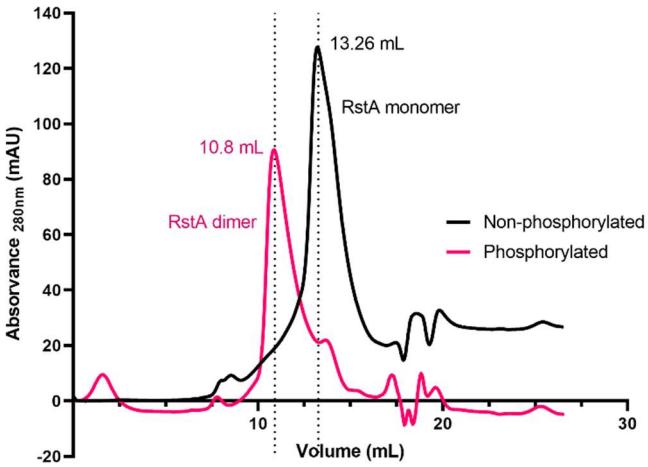

Figure 23 – Phosphorylation of RstA leads to dimerization. Analytical size exclusion chromatograms (Superose 12 10/300 GL) obtained for RstA in the absence (black) or presence (pink) of 10 mM acetylphosphate. Note that in the presence of acetylphosphate, RstA elutes first (10.8 mL), when compared to RstA not exposed to acetylphosphate (13.26 mL), suggesting that phosphorylation results in dimer formation.

Analysis of the size exclusion chromatogram (Figure 23) shows that RstA treated with acetylphosphate, and thus presumably phosphorylated, elutes first, than the untreated protein. This finding strongly suggests that phosphorylation of RstA leads to an increase in its molecular weight, most likely its dimerization, similarly to what has been observed for other RR [116, 123].

3.2.3 Phosphorylated RstA interacts with the promoter regions of *aip56, pbt, pnpA* and *omp19*

As discussed above, *Phdp* virulence is highly dependent on two toxins, AIP56 and PBT, whose expression is regulated by RstB (see section 3.1.2). Besides regulating *aip56* and *pbt* expression, we showed that RstB also regulates the expression of other *Phdp* secreted factors, including *pnpA*, *omp19* and *padA*. However, it is not known if RstA is also involved in these regulations, or if cross-talks between RstB and other TCSs are operating in these cases. To clarify this, we decided to investigate if RstA was able to bind to the promoter regions of the RstB-regulated genes.

We started by testing binding of RstA to the *aip56* promoter (Figure 24) and to assess the effect of phosphorylation in the formation of the RstA-DNA complex. For this, non-phosphorylated and phosphorylated RstA was incubated with *aip56 or* phospholipase *(pla)* promoter regions and subjected to EMSA (Figure 24). The *pla* promoter was chosen as a negative control because it has been found that in *Phdd*, *pla*, which is highly conserved in *Phdp,* is not regulated by RstA (Carlos R. Osorio personal communication).

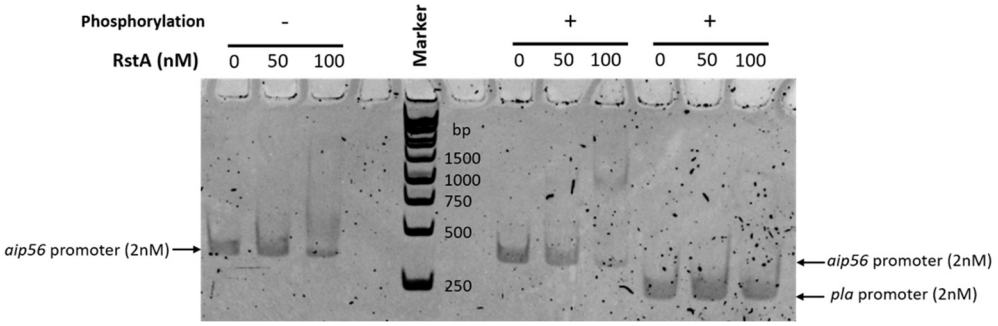

Figure 24 – EMSA assay showing that phosphorylated RstA binds specifically to the *aip56* promoter. 2 nM of *aip56* promoter were incubated with 0, 50 and 100 nM of RstA with and without 10 mM of acetylphosphate. 2 nM of *pla* promoter region incubated with RstA with 10 mM acetylphosphate was used as negative control. Note that phosphorylated RstA interacts, in a concentration dependent manner, with the aip56 promoter region, as evidenced by the shift upwards of DNA-containing band. This binding is specific since no shift occurred when phosphorylated RstA was incubated with the *pla* promoter region. Marker: GeneRuler 1 kb DNA ladder (Thermo Fisher Scientific).

The results of the EMSA show a "shift" upwards of the *aip56* promoter band after incubation with 100 nM RstA, pointing to the presence of a higher molecular weight complex, when compared to the free DNA. It should be noted that when the *aip56* promoter was incubated with untreated (i.e., non-phosphorylated) RstA no shift was observed, suggesting that efficient binding of RstA to target DNA requires RstA phosphorylation. Similarly, no shift was detected when acetylphosphate-treated (phosphorylated) RstA was incubated with the *pla* promoter, which demonstrates that RstA binding to the *aip56* promoter was specific.

After confirming specific binding of RstA to the *aip56* promoter region, we performed additional EMSAs to evaluate binding of RstA to the promoter regions of other RstB-regulated genes. Based on the data above suggesting that binding of RstA requires phosphorylation (Figure 24), we used in these assays acetylphosphate-treated RstA (Figure 25).

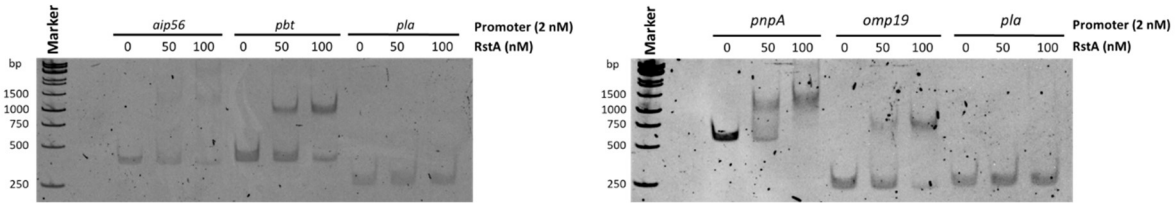

Figure 25 – RstA binds to the promoter regions of RstB-regulated genes *aip56*, *pbt*, *pnpA* and *omp19*. EMSA conducted using promoter regions of *aip56*, *pbt*, *pnpA* and *omp19*, incubated with increasing concentrations of

phosphorylated RstA (0, 50 and 100 nM). The *pla* promoter region was used as a negative control. Note that RstA bound to all promoter regions tested, except the promoter region of *pla*. Marker: GeneRuler 1 kb DNA ladder (Thermo Fisher Scientific).

As shown in Figure 25, RstA specifically bound to the promoter regions of *aip56*, *pbt*, *pnpA* and *omp19*, as concluded by the occurrence of shift upwards. As expected, no shift was observed with *pla* promoter. The results of these EMSAs suggest that RstA regulates the expression of *aip56*, *pbt*, *pnpA* and *omp19*. The fact that these genes are also regulated by RstB (Figures 16 and 17) indicates that regulation occurs by the canonical pathway of the RstAB TCS.

3.2.4 RstA interacts with the promoter regions of *padA* and *padB*

In order to investigate if RstB regulates the expression of PadA via the canonical pathway of the RstAB TCS, we conducted an EMSA assay, using the promoter region of *padA*. In parallel, we also tested the promoter region of *padB,* whose expression does not depend on RstB (Figure 18). The promoter regions of *pla* and *pbt* were used as negative and positive controls, respectively.

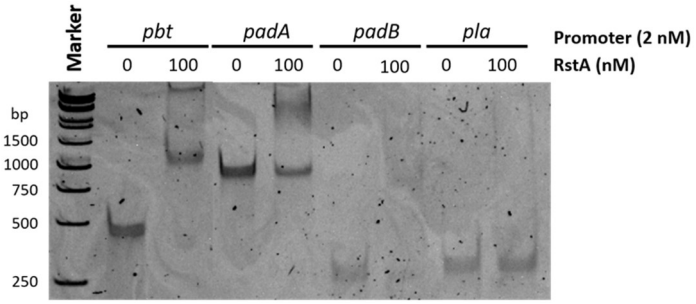

Figure 26 – RstA specifically binds to promoter region of *padA* and *padB*. EMSA conducted with 2 nM of promoter regions of *padA* and *padB* incubated with 0, 50 or 100 nM RstA in the presence of 10 mM acetyl phosphate. The *pla* and *pbt* promoter regions were used as negative and positive controls, respectively. Marker: GeneRuler 1 kb DNA ladder (Thermo Fisher Scientific).

As shown in Figure 26, a shift was observed both for the *padA* and *padB* promoters, suggesting that RstA is involved in the regulation of *padA* and *padB* expression. These results, together with the results presented above showing that RstB regulates the expression of *padA* but not *padB* (Figure 18), suggest that *padA* expression is regulated by the canonical RstAB pathway, whereas regulation of *padB* expression requires a cross-talk between RstAB and other unidentified TCS.

3.3 Identification of RstA residues required for DNA-binding

3.3.1 Prediction of key residues required for RstA-DNA interaction

Binding of RstA to DNA is a critical step for gene regulation. The binding region of response regulators is highly conserved across homologues, with slight variations that determine binding specificity. In order to predict the key residues involved in the binding of *Phdp* RstA to DNA, a model of *Phdp* RstA was generated using Phyre2 [131]. Superposition of *Phdp* RstA model with the structure of PhoP-DNA complex from *Mycobacterium tuberculosis* (PDB: 5ED4), in which the residues involved in the DNA-binding have been characterized [123], allowed to identify seven residues in *Phdp* RstA (R179, R187, R196, K201, R206, K207 and R223) that may play a key role in DNA interaction (Figure 27).

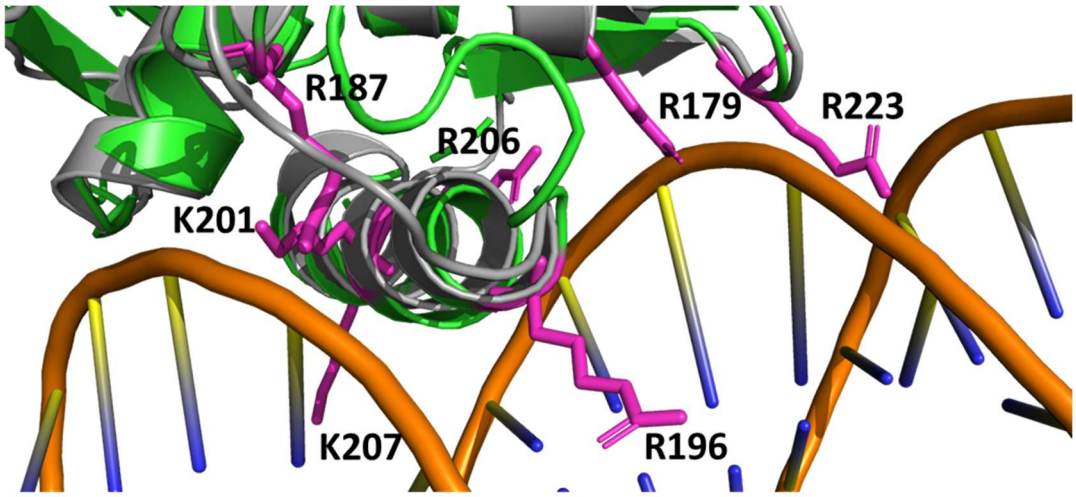

Figure 27 – RstA residues predicted to be involved in DNA binding. Cartoon representation of the superposition of RstA model generated by Phyre2 (green) with PhoP-DNA complex from *Mycobacterium tuberculosis* (gray; PDB:5ED4). Residues predicted to be involved in RstA-DNA binding (R179, R187, R196, K201, R206, K207 and R223) are represented by pink sticks.

A sequence alignment between *Phdp* RstA homologues, such as PhoP from *Mycobacterium tuberculosis* (MtbPhoP), AdeR from *Acinetobacter baumannii* (AdeR), and RstA from APEC (APECRstA), *Klebsiella pneumoniae* (KpRstA) and *Salmonella enterica* (SalerRstA), revealed that except for K201, all those residues are conserved across the five homologues (Figure 28).

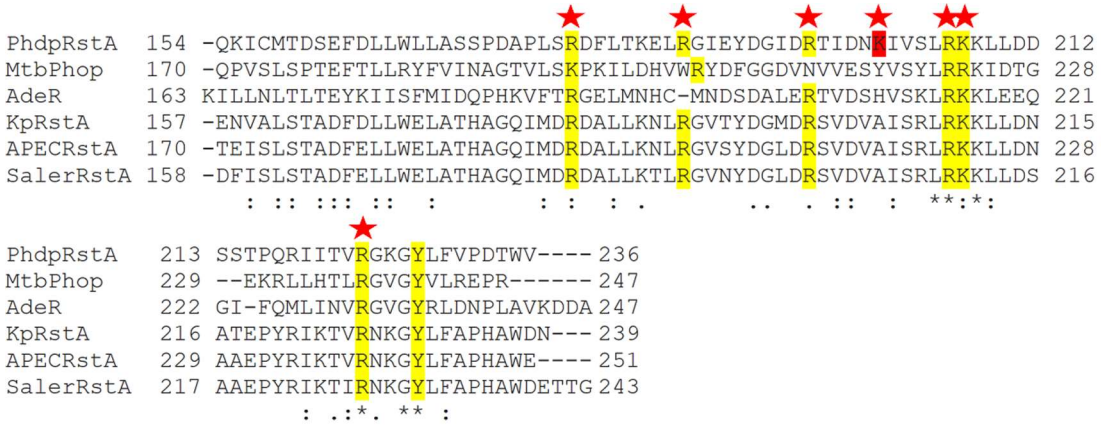

Figure 28 – Sequence alignment of multiple RstA homologues. Sequences shown belong to PhoP from *Mycobacterium tuberculosis* (MtbPhoP, Uniprot: P71814), AdeR from *Acinetobacter baumannii* (AdeR, Uniprot: E1A0Z5), and RstA from APEC (APECRstA, Uniprot: A0A0H2YZ82), from *Klebsiella penumoniae* (KpRstA, Uniprot: A6T8N1) and *Salmonella enterica* (SalerRstA, Uniprot: A0A379Q6Y2). Residues highlighted in yellow are conserved across the OmpR/PhoB subfamiliy and have been shown to play a role in DNA binding in MtbPhoP [123], AdeR [124] and KpRstA [116]. Residues highlighted with a red star are residues predicted to be involved in the formation of salt-bridges in *Phdp* RstA-DNA interaction. K201, which is not conserved, is highlighted in red.

3.3.2 Production of RstA mutants

To test if the 7 residues identified in *Phdp* RstA are involved in DNA-binding, we produced RstA versions in which each of those residues was substituted by an alanine The RstA mutants were expressed and purified as described in sections 2.9.5 to 2.9.8 for WT RstA.

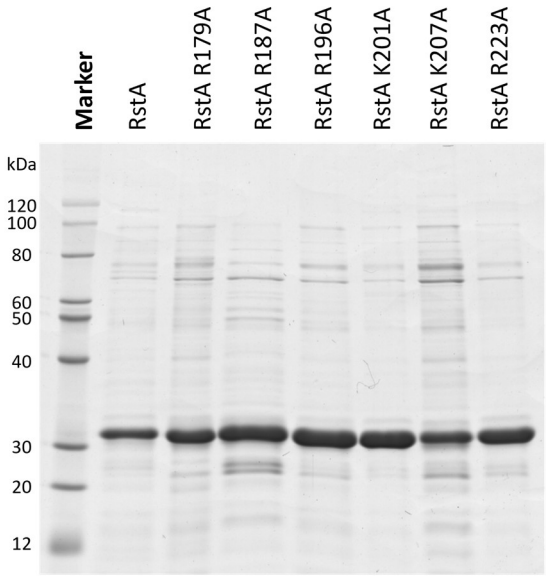

Figure 29 – SDS-PAGE of purified RstA mutants. Coomassie-blue stained SDS-PAGE gel of the final batches of the RstA proteins obtained after purification, dialysis and concentration. Each lane was loaded with 5 μg total protein. Purities estimated by densitometry: RstA (85%), R179A (79%), R187A (78%), R196A (91%), K201A (93%), K207A (62%), R223A (91%). Marker: GRS unstained protein ladder (GRiSP).

We were able to purify all mutants except R206A, which was insoluble. The obtained recombinant proteins were then tested by EMSA, using *pbt* promoter as a target DNA (Figure 30), to investigate if the mutations affected RstA-DNA interaction. This promoter was chosen because it leads to a clearer shift when compared to the other RstA targeted promoters tested (Figure 25).

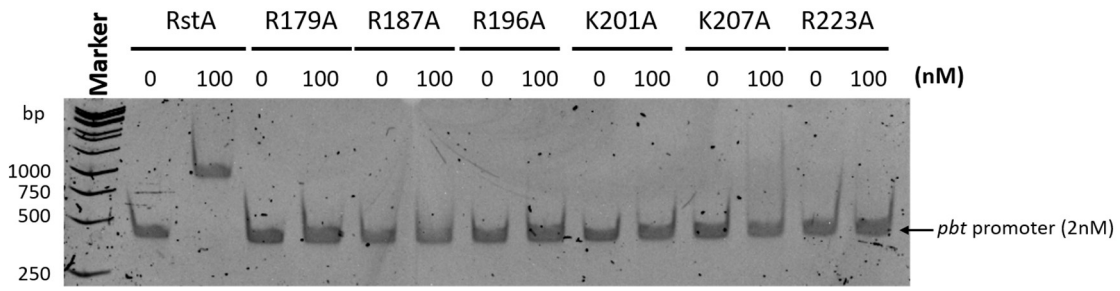

Figure 30 – Mutation of R179, R187, R196, K201, K207 and R223 impairs RstA-DNA binding. EMSA conducted using phosphorylated RstA or RstA mutants incubated with *pbt* promoter region. WT RstA was used as a positive control. Note that no shift occurred with RstA mutants, suggesting that the residues targeted by mutation are involved in the binding of RstA to DNA. Marker: GeneRuler 1 kb DNA ladder (Thermo Fisher Scientific).

Analysis of the EMSA results shows that DNA binding was abolished in all mutants, suggesting that all residues targeted by mutation are required for binding of RstA to DNA. To confirm that the inability of the RstA mutants to interact with the DNA was not due to incorrect structural conformation of the proteins, all mutants were analyzed by circular dichroism, to evaluate their secondary structure content (Figure 31).

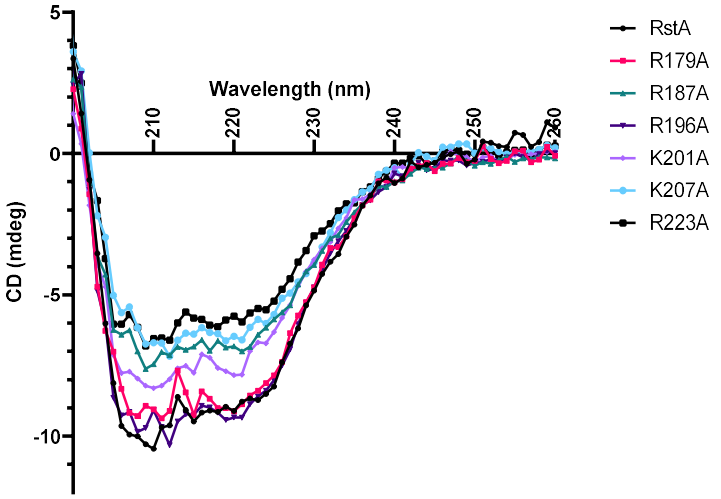

Figure 31 – Circular dichroism analysis of WT and RstA mutants. RstA and RstA mutants were dialyzed against 20 mM HEPES pH 7.0, 300 mM NaF, 10% (v/v) glycerol, 1 mM DTT. For circular dichroism, samples were diluted in 500 mM NaF to a final concentration of 100 µg/mL in a volume of 250 µL. Data were collected between 190 and 260 nm.

As shown in Figure 31, the circular dichroism curves of the RstA mutants are similar to the one of the WT RstA, indicating that the introduced substitutions did not affect the

secondary structure of the protein. This supports the conclusion that the mutation of these residues compromised the RstA-DNA interaction via binding impairment.

4. Discussion

Two-component regulatory systems (TCSs) are signal transduction pathways used in bacteria that have been show to play major roles in survival, virulence and cell growth [70]. They respond to different types of stimuli, ranging from salt concentrations or antimicrobial peptides to functional state of the cell envelope and intracellular metabolic signals [72, 139]. When activated, TCS regulate gene expression, by repression or activation, and, in some cases, cause changes in biochemical activities of certain proteins. Signal transduction by TCSs involves a cascade of phosphorylation/dephosphorylation reactions [73] that begins with the autophosphorylation of the SK in response to a specific stimulus [74, 75]. The phosphoryl group from the sensor kinase is then transferred to a conserved aspartate residue on the RR [74], leading to its dimerization and increasing the DNA binding affinity [73].

TCSs are not present in animals, but play major roles in bacteria, by regulating cell growth and fitness [94, 95], as well as the expression of virulence factors and drug-resistance related genes [96-98]. Therefore, they are prime candidates for the development of new antibacterial agents. Thus, it is highly relevant to study their structure and signal transduction mechanisms.

RstAB is a TCS from the OmpR/PhoB subfamily that is composed by the membrane embedded sensor kinase RstB, and the response regulator RstA [116, 117]. This TCS has been identified in various bacteria and has been shown to play a key role in virulence and sporulation [114, 115] but it has also been associated with the expression of efflux pumps involved in multidrug resistance and with resistance to nitrosative stress [112]. RstAB has also been shown to regulate the virulence of *Phdd*, by regulating the expression of its three major toxins Dly, PhlyP, and PhlyC [96], a polysaccharide capsule required for virulence, outer membrane proteins, and genes associated with antimicrobial resistance [79].

RstAB has been identified in *Phdp* (Unpublished data from FIV Group) but its role in regulating *Phdp* virulence has not been investigated. However it is likely that at least some genes will be differentially regulated by RstAB in the two subspecies, because *Phdp* has developed host-specific virulence factors, as well as an infection mechanisms that differs from the one of *Phdd* [126].

In order to understand if RstAB is important for *Phdp* virulence, we assessed the impact of *rstB* deletion for *Phdp* lethality in sea bass. This assay showed that deletion of *rstB* leads to a strong impairment in virulence, indicating that RstB is a key regulator of *Phdp* virulence (Figure 15). Although it would be interesting to complement these studies by

investigating the virulence role of RstA, this has not been possible because despite several attempts, the *rstA* deletion mutant could not be generated.

ECPs play a major role in *Phdp* virulence [11] and contain two virulence-related toxins: the apoptosis-inducing protein AIP56 [6] and the *Photobacterium* binary toxin, PBT, composed of PBTa and PBTb (Unpublished data from FIV Group). In this work, we showed that RstB regulates the expression of these toxins (Figure 16 and 17). Considering their major virulence roles, it is reasonable to speculate that their downregulation is responsible for the decreased virulence of the Δ*rstB* mutant. In addition to regulating expression of AIP56 and PBT, we showed that RstB regulates the expression of PnpA, a previously identified secreted protein [17], whose role in virulence remains unclear, as well as OMP19, a newly identified outer membrane protein that is highly abundant in outer membrane vesicles (Unpublished data from FIV Group) (Figure 16 and 17). It has recently been reported that laboratory *Phdp* strains, such as the MT1415 used in this work, lost some genes during manipulation *in vitro*, due to the instability of the virulence-related plasmid pPHDPT3 that, amongst many other genes, encodes a T3SS [69]. As such, it would be of the upmost importance to evaluate the role of RstB in the regulation of factors secreted by *Phdp* field isolates, because it could provide a more complete picture of the RstB regulated genes in this bacterium. Nevertheless, all field isolates of *Phdp* analyzed so far express AIP56 [140] and PBT, and it is expected that the regulation of these toxins by RstB is important for the virulence of these strains.

Recently, two putative trimeric autotransporter adhesins, PadA and PadB, that are not present in the MT1415 strain, were identified (Unpublished data from FIV group). Adhesins play a major role in virulence in many bacteria, mainly by mediating adhesion to host cells and tissues [43]. Although we predict that PadA and PadB play major virulence roles in *Phdp*, the fact that PadA and PadB are encoded in the unstable plasmid pPHDPT3 [69] complicated the characterization of their biological roles, as it was not possible to obtain isogenic mutants lacking these adhesins. However, we were able to study the role of RstB in the regulation of PadA and PadB expression, by complementing MT1415 WT and *ΔrstB* strains with plasmids encoding *padA* or *padB* under the control of their respective endogenous promoters. By comparing the levels of PadA and PadB expressed by WT and *ΔrstB* strains, we found that *rstB* deletion led to a drastic downregulation in the expression of PadA but did not affect expression of PadB (Figure 18). Although these results were obtained in an “artificial” system, the fact that *padA* and *padB* were under the control of their endogenous promoter strongly suggests that expression of *padA* in the field isolates is also regulated by RstB.

There are reports of cross-talks between TCS, including RstAB homologues [78, 104]. For example, there is evidence for a cross-talk between RstAB and RcsCDB in *S. Typhimurium*, showing that the STM1485 gene, can be regulated by RcsB or RstA under different conditions [104]. Thus, the fact that a gene is regulated by RstB does not necessarily means that it is also regulated by RstA. To investigate if the *Phdp* genes regulated by RstB were also regulated by RstA, we analyzed the interaction of RstA with the putative promoter regions of the RstB-regulated genes *aip56, pbt, pnpA, omp19, padA* and *padB*.

We started by optimizing the production and purification of RstA, to obtain the protein in an appropriate concentration and level of purity suitable for biochemical assays. A thermal shift assay allowed me to identify a a buffer in which RstA is stable (Figure 20), leading to the production of a more active and purer recombinant RstA protein (Figure 21).

Since it is known that phosphorylation is required for dimerization and/or to increase the binding affinity of RstA homologues, and the phosphorylation site is conserved in *Phdp* RstA (Figure 22), we developed an *in vitro* phosphorylation assay to investigate if phosphorylation led to dimerization of *Phdp* RstA. Comparison of the SEC elution times of non-phosphorylated and phosphorylated RstA strongly suggested that phosphorylation results in its dimerization (Figure 23). We then performed EMSAs to analyze the ability of phosphorylated and non-phosphorylated RstA to interact with the *aip56* promoter, showing that phosphorylation is required for DNA interaction (Figure 24). Phosphorylated RstA specifically interacted with the promoter region of the RstB-regulated genes *aip56*, *pbt*, *pnpA*, *omp19* and *padA* (Figure 25 and 26), which points to involvement of the canonical RstAB pathway in the regulation of these genes. Interestingly, RstA also interacted with the promoter region of *padB* (Figure 26), whose expression is RstB-independent, pointing to the occurrence of a possible cross-talk between RstA and a non-cognate sensor kinase. Further studies are undoubtably required to dissect the regulatory pathways that control expression of this *Phdp* putative adhesin.

To understand the molecular details underlying the RstA-DNA interaction, seven residues predicted to be involved in RstA-DNA interaction were identified (R179, R187, R196, K201, R206, K207 and R223), mutated to alanine, and the impact of the mutations in DNA-binding affinity assessed by performing EMSA. Mutant R206A was insoluble and thus, was excluded from this study. As expected, the mutation of R179, R187, R196, K201, K207 and R223 resulted in binding impairment, confirming that these residues play a major role in the formation of RstA-DNA complex.

5. Conclusion and future works

In this work we showed that RstAB plays a major role in regulating virulence and toxin expression in *Phdp*. We also showed that the RstAB TCS regulates expression of the peptidoglycan hydrolase PnpA, the outer membrane protein OMP19 and the trimeric autotransporter adhesin PadA, recently identified in a field isolated of *Phdp*.

Recently, TCSs have been used with success as drug targets. Considering the central role of RstAB in regulating major virulence factors of *Phdp*, it presents as a very promising target for developing anti-*Phdp* therapies. In this context, the here reported identification of residues required for RstA-DNA interaction is an asset for the development of binding inhibitors able to impair expression of RstA-dependent virulence genes. It is of note that the RstAB TCS is highly conserved in *Phdp* and *Phdd*. As such, compounds developed for *Phdp* RstAB should be effective against *Phdd* RstAB. This is of great importance because *Phdd* not only infects a wide variety of marine organisms, but also causes opportunistic and potentially fatal infections in humans. In the future, it would be important to develop studies aimed at identifying the *Phdp* RstA DNA binding box and at solving the 3D structure of RstA-DNA complex, as this could generate valuable information to guide virtual screening for compounds able to inhibit RstA-DNA interaction.

6. References

1. FAO, *The State of World Fisheries and Aquaculture 2020. Sustainability in action.* The State of World Fisheries and Aquaculture (SOFIA). Vol. 2020 - SOFIA 2020. 2020, Rome, Italy: FAO. #244.
2. Delalay, G., et al., *Characteristics of bacterial isolates in Swiss farmed and ornamental fish from a retrospective study from 2000 to 2017.* Schweiz Arch Tierheilkd, 2019. **161**(1): p. 43-57.
3. Romalde, J.L., *Photobacterium damselae subsp. piscicida: an integrated view of a bacterial fish pathogen.* Int Microbiol, 2002. **5**(1): p. 3-9.
4. Snieszko, S.F., et al., *PASTEURELLA SP. FROM AN EPIZOOTIC OF WHITE PERCH (ROCCUS AMERICANUS) IN CHESAPEAKE BAY TIDEWATER AREAS.* Journal of Bacteriology, 1964. **88**(6): p. 1814-1815.
5. Trůper, H.G. and L. De'Clari, *Taxonomic Note: Necessary Correction of Specific Epithets Formed as Substantives (Nouns) "in Apposition".* International Journal of Systematic and Evolutionary Microbiology, 1997. **47**(3): p. 908-909.
6. do Vale, A., et al., *AIP56, a novel plasmid-encoded virulence factor ofPhotobacterium damselaesubsp.piscicidawith apoptogenic activity against sea bass macrophages and neutrophils.* Molecular Microbiology, 2005. **58**(4): p. 1025-1038.
7. Noya, M., B. Magariños, and J. Lamas, *Interactions between peritoneal exudate cells (PECs) of gilthead seabream (Sparus aurata) and Pasteurella piscicida. A morphological study.* Aquaculture, 1995. **131**(1-2): p. 11-21.
8. Barnes, A.C., N.M. dos Santos, and A.E. Ellis, *Update on bacterial vaccines: Photobacterium damselae subsp. piscicida.* Dev Biol (Basel), 2005. **121**: p. 75-84.
9. do Vale, A., et al., *Systemic macrophage and neutrophil destruction by secondary necrosis induced by a bacterial exotoxin in a Gram-negative septicaemia.* 2007. **9**(4): p. 988-1003.
10. Magariños, B., A.E. Toranzo, and J.L. Romalde, *Phenotypic and pathobiological characteristics of Pasteurella piscicida.* Annual Review of Fish Diseases, 1996. **6**: p. 41-64.
11. Magarinos, B., et al., *Pathogenic activities of live cells and extracellular products of the fish pathogen Pasteurella piscicida.* Journal of General Microbiology, 1992. **138**(12): p. 2491-2498.

12. Silva, M.T., N.M.S. dos Santos, and A. do Vale, *AIP56: A Novel Bacterial Apoptogenic Toxin.* 2010. **2**(4): p. 905-918.
13. do Vale, A., et al., *The Apoptogenic Toxin AIP56 Is Secreted by the Type II Secretion System of Photobacterium damselae subsp. piscicida.* Toxins (Basel), 2017. **9**(11).
14. Silva, D.S., et al., *The Apoptogenic Toxin AIP56 Is a Metalloprotease A-B Toxin that Cleaves NF-κb P65.* PLoS Pathogens, 2013. **9**(2): p. e1003128.
15. Pereira, L.M.G., et al., *Intracellular Trafficking of AIP56, an NF-κB-Cleaving Toxin from Photobacterium damselae subsp. piscicida.* Infection and Immunity, 2014. **82**(12): p. 5270-5285.
16. Lee, C.-T., et al., *The opportunistic marine pathogenVibrio parahaemolyticusbecomes virulent by acquiring a plasmid that expresses a deadly toxin.* Proceedings of the National Academy of Sciences, 2015. **112**(34): p. 10798-10803.
17. Lisboa, J., et al., *A Secreted NlpC/P60 Endopeptidase from Photobacterium damselae subsp. piscicida Cleaves the Peptidoglycan of Potentially Competing Bacteria.* mSphere, 2021. **6**(1): p. e00736-20.
18. Cairo, G., F. Bernuzzi, and S. Recalcati, *A precious metal: Iron, an essential nutrient for all cells.* Genes & Nutrition, 2006. **1**(1): p. 25-39.
19. Monteith, A.J. and E.P. Skaar, *The impact of metal availability on immune function during infection.* Trends in Endocrinology & Metabolism, 2021. **32**(11): p. 916-928.
20. Sheldon, J.R., H.A. Laakso, and D.E. Heinrichs, *Iron Acquisition Strategies of Bacterial Pathogens.* Microbiol Spectr, 2016. **4**(2).
21. Magariños, B., et al., *Iron uptake by Pasteurella piscicida and its role in pathogenicity for fish.* Applied and Environmental Microbiology, 1994. **60**(8): p. 2990-2998.
22. Richard, K.L., B.R. Kelley, and J.G. Johnson, *Heme Uptake and Utilization by Gram-Negative Bacterial Pathogens.* Frontiers in cellular and infection microbiology, 2019. **9**: p. 81-81.
23. Lemos, M.L. and C.R. Osorio, *Heme, an iron supply for vibrios pathogenic for fish.* Biometals, 2007. **20**(3-4): p. 615-26.
24. Lemos, M.L. and M. Balado, *Iron uptake mechanisms as key virulence factors in bacterial fish pathogens.* Journal of Applied Microbiology, 2020. **129**(1): p. 104-115.
25. Noinaj, N., et al., *TonB-Dependent Transporters: Regulation, Structure, and Function.* Annual Review of Microbiology, 2010. **64**(1): p. 43-60.

26. Chu, B.C. and H.J. Vogel, *A structural and functional analysis of type III periplasmic and substrate binding proteins: their role in bacterial siderophore and heme transport.* Biol Chem, 2011. **392**(1-2): p. 39-52.
27. Tong, Y. and M. Guo, *Bacterial heme-transport proteins and their heme-coordination modes.* Archives of Biochemistry and Biophysics, 2009. **481**(1): p. 1-15.
28. Osorio, C.R., S. Juiz-Río, and M.L. Lemos, *A siderophore biosynthesis gene cluster from the fish pathogen Photobacterium damselae subsp. piscicida is structurally and functionally related to the Yersinia high-pathogenicity island.* Microbiology, 2006. **152**(11): p. 3327-3341.
29. Osorio, C.R., et al., *A Transmissible Plasmid-Borne Pathogenicity Island Confers Piscibactin Biosynthesis in the Fish Pathogen Photobacterium damselae subsp. piscicida.* Applied and environmental microbiology, 2015. **81**(17): p. 5867-5879.
30. Souto, A., et al., *Structure and Biosynthetic Assembly of Piscibactin, a Siderophore fromPhotobacterium damselaesubsp.piscicida, Predicted from Genome Analysis.* European Journal of Organic Chemistry, 2012. **2012**(29): p. 5693-5700.
31. Magarinos, B., et al., *Iron uptake by Pasteurella piscicida and its role in pathogenicity for fish.* Appl Environ Microbiol, 1994. **60**(8): p. 2990-8.
32. Osorio, C.R., S. Juiz-Río, and M.L. Lemos, *The ABC-transporter hutCD genes of Photobacterium damselae subsp. piscicida are essential for haem utilization as iron source and are expressed during infection in fish.* Journal of Fish Diseases, 2010. **33**(8): p. 649-655.
33. Ribet, D. and P. Cossart, *How bacterial pathogens colonize their hosts and invade deeper tissues.* Microbes and Infection, 2015. **17**(3): p. 173-183.
34. Moxon, E.R. and J.S. Kroll. *The Role of Bacterial Polysaccharide Capsules as Virulence Factors*. in *Bacterial Capsules*. 1990. Berlin, Heidelberg: Springer Berlin Heidelberg.
35. Kim, K.S., J.H. Kang, and A.S. Cross, *The role of capsular antigens in serum resistance and in vivo virulence of Escherichia coli.* FEMS Microbiology Letters, 1986. **35**(2-3): p. 275-278.
36. Howard, C.J. and A.A. Glynn, *The virulence for mice of strains of Escherichia coli related to the effects of K antigens on their resistance to phagocytosis and killing by complement.* Immunology, 1971. **20**(5): p. 767-77.
37. Häyrinen, J., D. Bitter-Suermann, and J. Flnne, *Interaction of meningococcal group B monoclonal antibody and its Fab fragment with α2-8-linked sialic acid*

polymers: Requirement of a long oligosaccharide segment for binding. Molecular Immunology, 1989. **26**(6): p. 523-529.

38. Bonet, R.N., et al., *Capsular polysaccharide expressed byPasteurella piscicidagrown in vitro.* FEMS Microbiology Letters, 1994. **124**(3): p. 285-289.
39. Magariños, B., et al., *Influence of the capsular layer on the virulence of Pasteurella piscicida for fish.* Microb Pathog, 1996. **21**(4): p. 289-97.
40. López-Dóriga, M.V., et al., *Invasion of fish epithelial cells by Photobacterium damselae subsp. piscicida: evidence for receptor specificity, and effect of capsule and serum.* Microbiology, 2000. **146**(1): p. 21-30.
41. Pizarro-Cerdá, J. and P. Cossart, *Bacterial Adhesion and Entry into Host Cells.* Cell, 2006. **124**(4): p. 715-727.
42. Kaper, J.B., J.P. Nataro, and H.L.T. Mobley, *Pathogenic Escherichia coli.* Nature Reviews Microbiology, 2004. **2**(2): p. 123-140.
43. Vo, J.L., et al., *Autotransporter Adhesins in Escherichia coli Pathogenesis.* PROTEOMICS, 2017. **17**(23-24): p. 1600431.
44. Busscher, H.J. and R.B.H.C. Der Mei, *Initial microbial adhesion is a determinant for the strength of biofilm adhesion.* FEMS Microbiology Letters, 1995. **128**(3): p. 229-234.
45. Chahales, P. and D.G. Thanassi, *Structure, Function, and Assembly of Adhesive Organelles by Uropathogenic Bacteria.* Microbiology Spectrum, 2015. **3**(5).
46. van Ulsen, P., et al., *Type V secretion: from biogenesis to biotechnology.* Biochim Biophys Acta, 2014. **1843**(8): p. 1592-611.
47. Henderson, I.R., et al., *Type V Protein Secretion Pathway: the Autotransporter Story.* Microbiology and Molecular Biology Reviews, 2004. **68**(4): p. 692-744.
48. Leyton, D.L., A.E. Rossiter, and I.R. Henderson, *From self sufficiency to dependence: mechanisms and factors important for autotransporter biogenesis.* Nature Reviews Microbiology, 2012. **10**(3): p. 213-225.
49. Driessen, A.J.M. and N. Nouwen, *Protein Translocation Across the Bacterial Cytoplasmic Membrane.* Annual Review of Biochemistry, 2008. **77**(1): p. 643-667.
50. Magarinos, B., et al., *Adherence and invasive capacities of the fish pathogenPasteurella piscicida.* FEMS Microbiology Letters, 1996. **138**(1): p. 29-34.
51. Acosta, F., et al., *Invasion and survival of Photobacterium damselae subsp. piscicida in non-phagocytic cells of gilthead sea bream, Sparus aurata L.* J Fish Dis, 2009. **32**(6): p. 535-41.

52. Meng, G., et al., *Structure of the outer membrane translocator domain of the Haemophilus influenzae Hia trimeric autotransporter.* The EMBO Journal, 2006. **25**(11): p. 2297-2304.
53. Hoiczyk, E., *Structure and sequence analysis of Yersinia YadA and Moraxella UspAs reveal a novel class of adhesins.* The EMBO Journal, 2000. **19**(22): p. 5989-5999.
54. Webb, B. and A. Sali, *Comparative Protein Structure Modeling Using MODELLER.* Current Protocols in Bioinformatics, 2016. **54**(1).
55. Büttner, D., *Protein Export According to Schedule: Architecture, Assembly, and Regulation of Type III Secretion Systems from Plant- and Animal-Pathogenic Bacteria.* Microbiology and Molecular Biology Reviews, 2012. **76**(2): p. 262-310.
56. Wagner, S., et al., *Bacterial type III secretion systems: a complex device for the delivery of bacterial effector proteins into eukaryotic host cells.* FEMS Microbiology Letters, 2018. **365**(19).
57. Zilkenat, S., et al., *Determination of the Stoichiometry of the Complete Bacterial Type III Secretion Needle Complex Using a Combined Quantitative Proteomic Approach.* Molecular & cellular proteomics : MCP, 2016. **15**(5): p. 1598-1609.
58. Park, D., et al., *Visualization of the type III secretion mediated Salmonella–host cell interface using cryo-electron tomography.* eLife, 2018. **7**.
59. Hueck, C.J., *Type III protein secretion systems in bacterial pathogens of animals and plants.* Microbiology and molecular biology reviews : MMBR, 1998. **62**(2): p. 379-433.
60. Lara-Tejero, M., et al., *A Sorting Platform Determines the Order of Protein Secretion in Bacterial Type III Systems.* Science, 2011. **331**(6021): p. 1188-1191.
61. Notti, R.Q., et al., *A common assembly module in injectisome and flagellar type III secretion sorting platforms.* Nature Communications, 2015. **6**(1): p. 7125.
62. Hu, B., et al., *In Situ Molecular Architecture of the Salmonella Type III Secretion Machine.* Cell, 2017. **168**(6): p. 1065-1074.e10.
63. Wagner, S., et al., *Organization and coordinated assembly of the type III secretion export apparatus.* Proceedings of the National Academy of Sciences, 2010. **107**(41): p. 17745-17750.
64. Broz, P., et al., *Function and molecular architecture of the Yersinia injectisome tip complex.* Molecular Microbiology, 2007. **65**(5): p. 1311-1320.
65. Botteaux, A., et al., *MxiC is secreted by and controls the substrate specificity of theShigella flexneritype III secretion apparatus.* Molecular Microbiology, 2009. **71**(2): p. 449-460.

66. Blocker, A.J., et al., *What's the point of the type III secretion system needle?* Proceedings of the National Academy of Sciences, 2008. **105**(18): p. 6507-6513.
67. Abushattal, S., et al., *Draft Genome Sequences of Photobacterium damselae subsp. piscicida SNW-8.1 and PP3, Two Fish-Isolated Strains Containing a Type III Secretion System.* Microbiology Resource Announcements, 2019. **8**(21).
68. Abushattal, S., A. Vences, and C.R. Osorio, *A virulence gene typing scheme for Photobacterium damselae subsp. piscicida, the causative agent of fish photobacteriosis, reveals a high prevalence of plasmid-encoded virulence factors and of type III secretion system genes.* Aquaculture, 2020. **521**: p. 735057.
69. Abushattal, S., A. Vences, and C.R. Osorio, *A Highly Unstable and Elusive Plasmid That Encodes the Type III Secretion System Is Necessary for Full Virulence in the Marine Fish Pathogen Photobacterium damselae subsp. piscicida.* International Journal of Molecular Sciences, 2022. **23**(9): p. 4729.
70. Skerker, J.M., et al., *Two-Component Signal Transduction Pathways Regulating Growth and Cell Cycle Progression in a Bacterium: A System-Level Analysis.* PLoS Biology, 2005. **3**(10): p. e334.
71. Groisman, E.A., *Feedback Control of Two-Component Regulatory Systems.* Annual Review of Microbiology, 2016. **70**(1): p. 103-124.
72. Stock, A.M., V.L. Robinson, and P.N. Goudreau, *Two-Component Signal Transduction.* Annual Review of Biochemistry, 2000. **69**(1): p. 183-215.
73. Zschiedrich, C.P., V. Keidel, and H. Szurmant, *Molecular Mechanisms of Two-Component Signal Transduction.* Journal of Molecular Biology, 2016. **428**(19): p. 3752-3775.
74. Bourret, R.B. and R.E. Silversmith, *Chapter Eleven - Measuring the Activities of Two-Component Regulatory System Phosphatases*, in *Methods in Enzymology*, K.N. Allen, Editor. 2018, Academic Press. p. 321-351.
75. Breland, E.J., A.R. Eberly, and M. Hadjifrangiskou, *An Overview of Two-Component Signal Transduction Systems Implicated in Extra-Intestinal Pathogenic E. coli Infections.* Frontiers in Cellular and Infection Microbiology, 2017. **7**.
76. Yamamoto, K., *The hierarchic network of metal-response transcription factors in Escherichia coli.* Bioscience, Biotechnology, and Biochemistry, 2014. **78**(5): p. 737-747.
77. Yamamoto, K., et al., *Functional Characterization in Vitro of All Two-component Signal Transduction Systems from Escherichia coli.* Journal of Biological Chemistry, 2005. **280**(2): p. 1448-1456.

78. Yoshida, M., A. Ishihama, and K. Yamamoto, *Cross talk in promoter recognition between six NarL-family response regulators of Escherichia coli two-component system.* Genes Cells, 2015. **20**(7): p. 601-12.
79. Matanza, X.M., et al., *The two-component system RstAB regulates production of a polysaccharide capsule with a role in virulence in the marine pathogen Photobacterium damselae subsp. damselae.* Environmental Microbiology, 2021.
80. Dutta, R., L. Qin, and M. Inouye, *Histidine kinases: Diversity of domain organization.* Molecular Microbiology, 1999. **34**(4): p. 633-640.
81. Deribe, Y.L., T. Pawson, and I. Dikic, *Post-translational modifications in signal integration.* Nature Structural & Molecular Biology, 2010. **17**(6): p. 666-672.
82. Su, Y., et al., *Methylation of PhoP by CheR Regulates Salmonella Virulence.* mBio, 2021. **12**(5): p. e02099-21.
83. Xue, J., et al., *Arginine GlcNAcylation and Activity Regulation of PhoP by a Type III Secretion System Effector in Salmonella.* Front Microbiol, 2021. **12**: p. 825743.
84. Wang, Y.-P., et al., *Arginine Methylation of MDH1 by CARM1 Inhibits Glutamine Metabolism and Suppresses Pancreatic Cancer.* Molecular Cell, 2016. **64**(4): p. 673-687.
85. Yang, X.-J. and E. Seto, *Lysine Acetylation: Codified Crosstalk with Other Posttranslational Modifications.* Molecular Cell, 2008. **31**(4): p. 449-461.
86. Kouzarides, T., *Acetylation: a regulatory modification to rival phosphorylation?* The EMBO Journal, 2000. **19**(6): p. 1176-1179.
87. Lee, J.S., et al., *Mutation in the Transcriptional Regulator PhoP Contributes to Avirulence of Mycobacterium tuberculosis H37Ra Strain.* Cell Host & Microbe, 2008. **3**(2): p. 97-103.
88. Ren, J., et al., *Acetylation of Lysine 201 Inhibits the DNA-Binding Ability of PhoP to Regulate Salmonella Virulence.* PLOS Pathogens, 2016. **12**(3): p. e1005458.
89. Bajaj, V., et al., *Co-ordinate regulation of Salmonella typhimurium invasion genes by environmental and regulatory factors is mediated by control of hilA expression.* Molecular Microbiology, 1996. **22**(4): p. 703-714.
90. Bijlsma, J.J.E. and E.A. Groisman, *The PhoP/PhoQ system controls the intramacrophage type three secretion system of Salmonella enterica.* Molecular Microbiology, 2005. **57**(1): p. 85-96.
91. Garbom, S., et al., *Phenotypic characterization of a virulence-associated protein, VagH, of Yersinia pseudotuberculosis reveals a tight link between VagH and the type III secretion system.* Microbiology, 2007. **153**(5): p. 1464-1473.
92. Yang, D.C.H., et al., *Outer Membrane Protein OmpB Methylation May Mediate Bacterial Virulence.* Trends Biochem Sci, 2017. **42**(12): p. 936-945.

93. Sprung, R., et al., *Identification and Validation of Eukaryotic Aspartate and Glutamate Methylation in Proteins.* Journal of Proteome Research, 2008. **7**(3): p. 1001-1006.
94. Terceti, M.S., et al., *The RstAB System Impacts Virulence, Motility, Cell Morphology, Penicillin Tolerance and Production of Type II Secretion System-Dependent Factors in the Fish and Human Pathogen Photobacterium damselae subsp. damselae.* Frontiers in Microbiology, 2019. **10**.
95. Murret-Labarthe, C., et al., *New Roles for Two-Component System Response Regulators of Salmonella enterica Serovar Typhi during Host Cell Interactions.* Microorganisms, 2020. **8**(5): p. 722.
96. Terceti, M.S., et al., *rstB Regulates Expression of the Photobacterium damselae subsp. damselae Major Virulence Factors Damselysin, Phobalysin P and Phobalysin C.* Frontiers in Microbiology, 2017. **08**.
97. Lee, Y.-T., et al., *AdeABC Efflux Pump Controlled by AdeRS Two Component System Conferring Resistance to Tigecycline, Omadacycline and Eravacycline in Clinical Carbapenem Resistant Acinetobacter nosocomialis.* Frontiers in Microbiology, 2020. **11**(2678).
98. Lu, H.-F., et al., *PhoPQ two-component regulatory system plays a global regulatory role in antibiotic susceptibility, physiology, stress adaptation, and virulence in Stenotrophomonas maltophilia.* BMC Microbiology, 2020. **20**(1).
99. Hirakawa, H., et al., *Progress Overview of Bacterial Two-Component Regulatory Systems as Potential Targets for Antimicrobial Chemotherapy.* Antibiotics, 2020. **9**(10): p. 635.
100. Hilliard, J.J., et al., *Multiple Mechanisms of Action for Inhibitors of Histidine Protein Kinases from Bacterial Two-Component Systems.* Antimicrobial Agents and Chemotherapy, 1999. **43**(7): p. 1693-1699.
101. Stephenson, K., Y. Yamaguchi, and J.A. Hoch, *The Mechanism of Action of Inhibitors of Bacterial Two-component Signal Transduction Systems.* Journal of Biological Chemistry, 2000. **275**(49): p. 38900-38904.
102. Gilmour, R., et al., *New Class of Competitive Inhibitor of Bacterial Histidine Kinases.* Journal of Bacteriology, 2005. **187**(23): p. 8196-8200.
103. Trouillon, J., et al., *Determination of the two-component systems regulatory network reveals core and accessory regulations across Pseudomonas aeruginosa lineages.* Nucleic Acids Research, 2021. **49**(20): p. 11476-11490.
104. Torrez Lamberti, M.F., et al., *Cross-talk between the RcsCDB and RstAB systems to control STM1485 gene expression in Salmonella Typhimurium during acid-resistance response.* Biochimie, 2019. **160**: p. 46-54.

105. Ho, Y.H., T.C. Sung, and C.S. Chen, *Lactoferricin B inhibits the phosphorylation of the two-component system response regulators BasR and CreB.* Mol Cell Proteomics, 2012. **11**(4): p. M111.014720.
106. Roychoudhury, S., et al., *Inhibitors of two-component signal transduction systems: inhibition of alginate gene activation in Pseudomonas aeruginosa.* Proceedings of the National Academy of Sciences, 1993. **90**(3): p. 965-969.
107. Hirakawa, H., et al., *In vitro activity of AST-120 that suppresses indole signaling in Escherichia coli, which attenuates drug tolerance and virulence.* PLOS ONE, 2020. **15**(4): p. e0232461.
108. Hirakawa, H., et al., *Indole induces the expression of multidrug exporter genes in Escherichia coli.* Molecular Microbiology, 2004. **55**(4): p. 1113-1126.
109. Hirakawa, H., et al., *Secreted indole serves as a signal for expression of type III secretion system translocators in enterohaemorrhagic Escherichia coli O157:H7.* Microbiology, 2009. **155**(2): p. 541-550.
110. Gutierrez, J.A., et al., *Transition state analogs of 5'-methylthioadenosine nucleosidase disrupt quorum sensing.* Nature Chemical Biology, 2009. **5**(4): p. 251-257.
111. Xavier, K.B. and B.L. Bassler, *LuxS quorum sensing: more than just a numbers game.* Curr Opin Microbiol, 2003. **6**(2): p. 191-7.
112. Li, D.Y., et al., *The Two-Component System RstA/RstB Regulates Expression of Multiple Efflux Pumps and Influences Anaerobic Nitrate Respiration in Pseudomonas fluorescens.* mSystems, 2021. **0**(0): p. e0091121.
113. Edwards, A.N., B.R. Anjuwon-Foster, and S.M. McBride, *RstA Is a Major Regulator of Clostridioides difficile Toxin Production and Motility.* mBio, 2019. **10**(2).
114. Gao, Q., et al., *Transcriptional analysis of RstA/RstB in avian pathogenic Escherichia coli identifies its role in the regulation of hdeD-mediated virulence and survival in chicken macrophages.* Veterinary Microbiology, 2020. **241**: p. 108555.
115. Edwards, A.N., E.G. Krall, and S.M. McBride, *Strain-Dependent RstA Regulation of Clostridioides difficile Toxin Production and Sporulation.* Journal of Bacteriology, 2020. **202**(2).
116. Li, Y.-C., et al., *Structural dynamics of the two-component response regulator RstA in recognition of promoter DNA element.* Nucleic Acids Research, 2014. **42**(13): p. 8777-8788.

117. Draughn, G.L., et al., *The Structure of the Biofilm-controlling Response Regulator BfmR from Acinetobacter baumannii Reveals Details of Its DNA-binding Mechanism.* Journal of Molecular Biology, 2018. **430**(6): p. 806-821.
118. Ogasawara, H., et al., *Genomic SELEX Search for Target Promoters under the Control of the PhoQP-RstBA Signal Relay Cascade.* 2007. **189**(13): p. 4791-4799.
119. Ogasawara, H., et al., *Genomic SELEX Search for Target Promoters under the Control of the PhoQP-RstBA Signal Relay Cascade.* Journal of Bacteriology, 2007. **189**(13): p. 4791-4799.
120. Okamura, H., et al., *Structural comparison of the PhoB and OmpR DNA-binding/transactivation domains and the arrangement of PhoB molecules on the phosphate box.* J Mol Biol, 2000. **295**(5): p. 1225-36.
121. Gurlie, R., T.H. Duong, and K. Zakrzewska, *The role of DNA-protein salt bridges in molecular recognition: a model study.* Biopolymers, 1999. **49**(4): p. 313-27.
122. Jelesarov, I. and A. Karshikoff, *Defining the role of salt bridges in protein stability.* Methods Mol Biol, 2009. **490**: p. 227-60.
123. He, X., L. Wang, and S. Wang, *Structural basis of DNA sequence recognition by the response regulator PhoP in Mycobacterium tuberculosis.* 2016. **6**: p. 24442.
124. Wen, Y., et al., *Mechanistic insight into how multidrug resistant Acinetobacter baumannii response regulator AdeR recognizes an intercistronic region.* Nucleic Acids Res, 2017. **45**(16): p. 9773-9787.
125. Perez, J.C., et al., *Evolution of a Bacterial Regulon Controlling Virulence and Mg2+ Homeostasis.* PLoS Genetics, 2009. **5**(3): p. e1000428.
126. Baseggio, L., et al., *The Evolution of a Specialized, Highly Virulent Fish Pathogen through Gene Loss and Acquisition of Host-Specific Survival Mechanisms.* Applied and Environmental Microbiology, 2022. **0**(0): p. e00222-22.
127. Pinheiro, J., et al., *Listeria monocytogenesencodes a functional ESX-1 secretion system whose expression is detrimental toin vivoinfection.* Virulence, 2017. **8**(6): p. 993-1004.
128. Bustin, S.A., et al., *The MIQE Guidelines: Minimum Information for Publication of Quantitative Real-Time PCR Experiments.* Clinical Chemistry, 2009. **55**(4): p. 611-622.
129. Consortium, T.U., *UniProt: the universal protein knowledgebase in 2021.* Nucleic Acids Research, 2020. **49**(D1): p. D480-D489.
130. McWilliam, H., et al., *Analysis Tool Web Services from the EMBL-EBI.* Nucleic Acids Research, 2013. **41**(W1): p. W597-W600.

131. Kelley, L.A., et al., *The Phyre2 web portal for protein modeling, prediction and analysis.* Nature Protocols, 2015. **10**(6): p. 845-858.
132. Asif, A., et al., *Revisiting the Mechanisms Involved in Calcium Chloride Induced Bacterial Transformation.* Frontiers in Microbiology, 2017. **8**.
133. Froger, A. and J.E. Hall, *Transformation of Plasmid DNA into E. coli Using the Heat Shock Method.* Journal of Visualized Experiments, 2007(6).
134. Wilkins, M.R., et al., *Protein identification and analysis tools in the ExPASy server.* Methods Mol Biol, 1999. **112**: p. 531-52.
135. Zschiedrich, C.P., V. Keidel, and H. Szurmant, *Molecular Mechanisms of Two-Component Signal Transduction.* J Mol Biol, 2016. **428**(19): p. 3752-75.
136. Bourret, R.B., *Receiver domain structure and function in response regulator proteins.* Current Opinion in Microbiology, 2010. **13**(2): p. 142-149.
137. Lukat, G.S., et al., *Phosphorylation of bacterial response regulator proteins by low molecular weight phospho-donors.* Proceedings of the National Academy of Sciences, 1992. **89**(2): p. 718-722.
138. Wolfe, A.J., *Physiologically relevant small phosphodonors link metabolism to signal transduction.* Current Opinion in Microbiology, 2010. **13**(2): p. 204-209.
139. Mascher, T., J.D. Helmann, and G. Unden, *Stimulus Perception in Bacterial Signal-Transducing Histidine Kinases.* Microbiology and Molecular Biology Reviews, 2006. **70**(4): p. 910-938.
140. Freitas, I.L., et al., *Susceptibility of Sea Bream (Sparus aurata) to AIP56, an AB-Type Toxin Secreted by Photobacterium damselae subsp. piscicida.* Toxins, 2022. **14**(2): p. 119.

7. Annex

Annex 1: Constructs used in this study and corresponding primers

Construct	Description	Sequence of recombinant protein	Primers used for cloning
pET28_RstA_FL	pET28 vector with Phdp RstA cloned into NcoI/XhoI restriction sites in frame with a C-terminal 6 His-tag; the LE amino-acids (corresponding to XhoI restriction site) were introduced between V235 and the C-terminal His-tag (already present in pET28 vector).	MGTETYSLLIIEDDLKLQQMLADYFLTQGFTVQTHSDGNGAIELL ESSNPDIVLLDLMLPGNDGLTICRQVRGKYQGKLMMLTASHD DFDHVAALEIGADDYVVKPIKPRVLLARMRMLLRRAKTQPNA PVNQNILNYGELTLHKNRKLCELSGQKICMTDSEFDLLWLLASS PDAPLSRDFLTKELRGIEYDGIDRTIDNKIVSLRKKLLDDSSTPQR IITVRGKGYLFVPDTWVLEHHHHHH	RstA_M1_V235_NcoI_FW NcoI 5' GCG CC ATG GGC ACA GAG ACT TAT TCA C 3' RstARvXhoI XhoI 5' GAG CTC GAG TAC CCA CGT ATC TGG AAC G 3'
pET28_RstA_FL^{R179A}	Mutation of R179 to alanine was achieved by site-directed mutagenesis by inverse PCR using Q5 high fidelity DNA polymerase and pET28_RstA_FL as a template; Both primers are phosphorylated at 5'	MATHNHNHLGCIRTMTETYSLLIIEDDLKLQQMLADYFLTQGFT VQTHSDGNGAIELIESSNPDIVLLDLMLPGNDGLTICRQVRGKY QGKLMMLTASHDDFDHVAALEIGADDYVVKPIKPRVLLARMR MLLRRAKTQPNAPVNQNILNYGELTLHKNRKLCELSGQKICMT DSEFDLLWLASSPDAPLSADFLTKELRGIEYDGIDRTIDNKIVSL RKKLLDDSSTPQRITVRGKGYLFVPDTWVLEHHHHHH	FW_RstA_R179A 5' [P] CT GAT GCA CCA TTA TCT GCA GAT TTT TTA ACT AAA G 3' RV_RstA_P173 5'[P] G AGA ACT TGC TAA TAA CCA TAA CAA ATC 3'
pET28_RstA_FL^{R187A}	Mutation of R187 to alanine was achieved by site-directed mutagenesis by inverse PCR using Q5 high fidelity DNA polymerase and pET28_RstA_FL as a template; Both primers are phosphorylated at 5'	MATHNHNHLGCIRTMTETYSLLIIEDDLKLQQMLADYFLTQGFT VQTHSDGNGAIELIESSNPDIVLLDLMLPGNDGLTICRQVRGKY QGKLMMLTASHDDFDHVAALEIGADDYVVKPIKPRVLLARMR MLLRRAKTQPNAPVNQNILNYGELTLHKNRKLCELSGQKICMT DSEFDLLWLASSPDAPLSRDFLTKELAGIEYDGIDRTIDNKIVSL RKKLLDDSSTPQRITVRGKGYLFVPDTWVLEHHHHHH	FW_RstA_G193 5' [P] G ATT GAT AGA ACC ATT GAT AAT AAG ATT GTG AGT C 3' RV2_RstA_R187A 5' [P] CC ATC ATA TTC AAT GCC GGC TAA TTC TTT AGT TAA AAA ATC AC 3'
pET28_RstA_FL^{R196A}	Mutation of R196 to alanine was achieved by site-directed mutagenesis by inverse PCR using Q5 high fidelity DNA polymerase and pET28_RstA_FL as a template; Both primers are phosphorylated at 5'	MATHNHNHLGCIRTMTETYSLLIIEDDLKLQQMLADYFLTQGFT VQTHSDGNGAIELIESSNPDIVLLDLMLPGNDGLTICRQVRGKY QGKLMMLTASHDDFDHVAALEIGADDYVVKPIKPRVLLARMR MLLRRAKTQPNAPVNQNILNYGELTLHKNRKLCELSGQKICMT DSEFDLLWLASSPDAPLSRDFLTKELRGIEYDGIDATIDNKIVSL RKKLLDDSSTPQRITVRGKGYLFVPDTWVLEHHHHHH	FW_RstA_R196A 5' [P] GCC ACC ATT GAT AAT AAG ATT GTG AGT C 3' RV_RstA_R196A 5' [P] ATC AAT CCC ATC ATA TTC AAT GCC GCG 3'

Annex 1 (continuation): Constructs used in this study and corresponding primers

Construct	Description	Sequence of recombinant protein	Primers used for doning
pET28_RstA_FL ^{K201A}	Mutation of K201 to alanine was achieved by site-directed mutagenesis by inverse PCR using Q5 high fidelity DNA polymerase and pET28_RstA_FL as a template; Both primers are phosphorylated at 5'	MATHNHNHLGCIRTMTETYSLLIEDDLKLQQMLADYFLTQGFT VQTHSDGNGAIELIESSNPDIVLLDLMLPGNDGLTICRQVRGKY QGKLMMLTASHDDFDHVAALEIGADDYVVKPIKPRVLLARMR MLLRRAKTQPNAPVNQNILNYGELTLHKNRKLCELSGQKICMT DSEFDLLWLLASSPDAPLSRDFLTKELRGIEYDGIDRTIDNAIVSL RKKLLDDSSTPQRIITVRGKGYLFVPDTWVLEHHHHHH	FW_RstA_R206 5' [P] GG AAA AAG CTG TTA GAC GAT TCT TCA AC 3' RV_RstA_K201A 5' [P] G TAG ACT CAC AAT GGC ATT ATC AAT GG 3'
pET28_RstA_FL ^{R206A}	Mutation of R206 to alanine was achieved by site-directed mutagenesis by inverse PCR using Q5 high fidelity DNA polymerase and pET28_RstA_FL as a template; Both primers are phosphorylated at 5'	MATHNHNHLGCIRTMTETYSLLIEDDLKLQQMLADYFLTQGFT VQTHSDGNGAIELIESSNPDIVLLDLMLPGNDGLTICRQVRGKY QGKLMMLTASHDDFDHVAALEIGADDYVVKPIKPRVLLARMR MLLRRAKTQPNAPVNQNILNYGELTLHKNRKLCELSGQKICMT DSEFDLLWLLASSPDAPLSRDFLTKELRGIEYDGIDRTIDNKIVSL AKKLLDDSSTPQRIITVRGKGYLFVPDTWVLEHHHHHH	FW_RstA_R206A 5' [P] GCC AAA AAG CTG TTA GAC GAT TCT TCA ACT C 3' RV_RstA_R206A 5' [P] TAG ACT CAC AAT CTT ATT ATC AAT GG 3'
pET28_RstA_FL ^{K207A}	Mutation of K207 to alanine was achieved by site-directed mutagenesis by inverse PCR using Q5 high fidelity DNA polymerase and pET28_RstA_FL as a template; Both primers are phosphorylated at 5'	MATHNHNHLGCIRTMTETYSLLIEDDLKLQQMLADYFLTQGFT VQTHSDGNGAIELIESSNPDIVLLDLMLPGNDGLTICRQVRGKY QGKLMMLTASHDDFDHVAALEIGADDYVVKPIKPRVLLARMR MLLRRAKTQPNAPVNQNILNYGELTLHKNRKLCELSGQKICMT DSEFDLLWLLASSPDAPLSRDFLTKELRGIEYDGIDRTIDNKIVSL RAKLLDDSSTPQRIITVRGKGYLFVPDTWVLEHHHHHH	FW_RstA_D212 5' [P] GAT TCT TCA ACT CCA CAG CGA ATT ATT ACT G 3' RV_RstA_K207A 5' [P] GTC TAA CAG CTT GGC CCG TAG ACT CAC AAT C 3'
pET28_RstA_FL ^{R223A}	Mutation of R223 to alanine was achieved by site-directed mutagenesis by inverse PCR using Q5 high fidelity DNA polymerase and pET28_RstA_FL as a template; Both primers are phosphorylated at 5'	MATHNHNHLGCIRTMTETYSLLIEDDLKLQQMLADYFLTQGFT VQTHSDGNGAIELIESSNPDIVLLDLMLPGNDGLTICRQVRGKY QGKLMMLTASHDDFDHVAALEIGADDYVVKPIKPRVLLARMR MLLRRAKTQPNAPVNQNILNYGELTLHKNRKLCELSGQKICMT DSEFDLLWLLASSPDAPLSRDFLTKELRGIEYDGIDRTIDNKIVSL RKKLLDDSSTPQRIITVAGKGYLFVPDTWVLEHHHHHH	FW_RstA_R223A 5' [P] GA ATT ATT ACT GTC GCA GGT AAG GGC TAT TTA TTC G 3' RV_RstA_R218 5' [P] G CTG TGG AGT TGA AGA ATC GTC TAA C 3'

Annex 2: Thermal shift plates . Upon addition of protein, concentrations displayed are halved.

Plate A

Wells	1	2	3	4	5	6	7	8	9	10	11	12
A No Salt	Na Acetate 200 mM pH 4	Na Acetate 200 mM pH 4.5	Na Citrate 200 mM pH 5	Na Citrate 200 mM pH 5.5	Na Cacodylate 200 mM pH 6	Na Cacodylate 200 mM pH 6.5	Hepes 200 mM pH 7	Hepes 200 mM pH 7.5	Tris 200 mM pH 8	Tris 200 mM pH 8.5	CHES 200 mM pH 9	CHES 200 mM pH 9.5
B No Salt	Acid citric 200 mM pH 4	Acid citric 200 mM pH 4.5	Acid citric 200 mM pH 5	Acid citric 200 mM pH 5.5	MES 200 mM pH 6	Bis-Tris 200 mM pH 6.5	MOPS 200 mM pH 7	Bis-Tris Propane 200 mM pH 7.5	Tricine 200 mM pH 8	Bicine 200 mM pH 8.5	Glycine 200 mM pH 9	CAPSO 200 mM pH 9.5
C 200 mM NaCl	Na Acetate 200 mM pH 4	Na Acetate 200 mM pH 4.5	Na Citrate 200 mM pH 5	Na Citrate 200 mM pH 5.5	Na Cacodylate 200 mM pH 6	Na Cacodylate 200 mM pH 6.5	Hepes 200 mM pH 7	Hepes 200 mM pH 7.5	Tris 200 mM pH 8	Tris 200 mM pH 8.5	CHES 200 mM pH 9	CHES 200 mM pH 9.5
D 200 mM NaCl	Acid citric 200 mM pH 4	Acid citric 200 mM pH 4.5	Acid citric 200 mM pH 5	Acid citric 200 mM pH 5.5	MES 200 mM pH 6	Bis-Tris 200 mM pH 6.5	MOPS 200 mM pH 7	Bis-Tris Propane 200 mM pH 7.5	Tricine 200 mM pH 8	Bicine 200 mM pH 8.5	Glycine 200 mM pH 9	CAPSO 200 mM pH 9.5
E 400 mM NaCl	Na Acetate 200 mM pH 4	Na Acetate 200 mM pH 4.5	Na Citrate 200 mM pH 5	Na Citrate 200 mM pH 5.5	Na Cacodylate 200 mM pH 6	Na Cacodylate 200 mM pH 6.5	Hepes 200 mM pH 7	Hepes 200 mM pH 7.5	Tris 200 mM pH 8	Tris 200 mM pH 8.5	CHES 200 mM pH 9	CHES 200 mM pH 9.5
F 400 mM NaCl	Acid citric 200 mM pH 4	Acid citric 200 mM pH 4.5	Acid citric 200 mM pH 5	Acid citric 200 mM pH 5.5	MES 200 mM pH 6	Bis-Tris 200 mM pH 6.5	MOPS 200 mM pH 7	Bis-Tris Propane 200 mM pH 7.5	Tricine 200 mM pH 8	Bicine 200 mM pH 8.5	Glycine 200 mM pH 9	CAPSO 200 mM pH 9.5
G 1000 mM NaCl	Na Acetate 200 mM pH 4	Na Acetate 200 mM pH 4.5	Na Citrate 200 mM pH 5	Na Citrate 200 mM pH 5.5	Na Cacodylate 200 mM pH 6	Na Cacodylate 200 mM pH 6.5	Hepes 200 mM pH 7	Hepes 200 mM pH 7.5	Tris 200 mM pH 8	Tris 200 mM pH 8.5	CHES 200 mM pH 9	CHES 200 mM pH 9.5
H 1000 mM NaCl	Acid citric 200 mM pH 4	Acid citric 200 mM pH 4.5	Acid citric 200 mM pH 5	Acid citric 200 mM pH 5.5	MES 200 mM pH 6	Bis-Tris 200 mM pH 6.5	MOPS 200 mM pH 7	Bis-Tris Propane 200 mM pH 7.5	Tricine 200 mM pH 8	Bicine 200 mM pH 8.5	Glycine 200 mM pH 9	CAPSO 200 mM pH 9.5

Plate B

Wells	1	2	3	4	5	6	7	8	9	10	11	12
A	2.5% (v/v) Glycerol	5% (v/v) Glycerol	10% (v/v) Glycerol	15% (v/v) Glycerol	20% (v/v) Glycerol	AMP 10 mM + 10 mM $MgCl_2$	ADP 10 mM + 10 mM $MgCl_2$	ATP 10 mM + 10 mM $MgCl_2$	AMPPcP 10 mM + 10 mM $MgCl_2$	GMP 10 mM + 10 mM $MgCl_2$	GDP 10 mM + 10 mM $MgCl_2$	GTP 10 mM + 10 mM $MgCl_2$
B	GMPPcP 10 mM + 10 mM $MgCl_2$	CMP 10 mM + 10 mM $MgCl_2$	NADH 10 mM	NADPH 10 mM	FAD 10 mM	Riboflavin 10 mM	SAM 10 mM	Acetyl CoA 10 mM	Phytic acid 10 mM	PLP 10 mM	$CaCl_2$ 10 mM	$MgCl_2$ 10 mM
C	$MnCl_2$ 10 mM	$ZnCl_2$ 10 mM	$FeCl_2$ 10 mM	$NiCl_2$ 10 mM	$ZnSO_4$ 10 mM	KBr 10 mM	Glucose 10 mM	2-oxoglutarate 10 mM	3% (v/v) DMSO	DTT 1 mM	DTT 5 mM	EDTA 5 mM
D	TCEP 5 mM	β-mercaptoethanol 1 mM	β-mercaptoethanol 5 mM	Urea 10 mM	CHAPS 5 mM	0.2% (v/v) Triton X-100	1% (v/v) Triton X-100	2% (v/v) Triton X-100	5% (v/v) Triton X-100	Glycine 10 mM	Taurine 10 mM	Spermidine 10 mM
E	Bétaine 10 mM	L-Proline 10 mM	L-Leucine 10 mM	L-Arginine 10 mM	$NaNO_3$ 200 mM	NaSCN 200 mM	Na_2SO_4 200 mM	$(NH_4)_2SO_4$ 200 mM	NH4Cl 200 mM	Imidazole 200 mM	Imidazole 600 mM	$C_4H_4KNaO_6$ 200 mM
F	Na Iodide 200 mM	Na Formate 200 mM	Na Acetate 200 mM	Na Malonate 200 mM	$C_4H_4Na_2O_6$ 200 mM	Cadmium Acetate 200 mM	NaF 200 mM	KCl 200 mM	LiCl 200 mM	NaBr 200 mM	H_2O	Previous buffer
G	NaCl 50 mM	NaCl 100 mM	NaCl 150 mM	NaCl 200 mM	NaCl 300 mM	NaCl 400 mM	NaCl 500 mM	NaCl 600 mM	NaCl 700 mM	NaCl 800 mM	NaCl 900 mM	NaCl 1000 mM

Annex 3: DNA segments used in EMSA and corresponding primers

DNA	Description	DNA sequence	Primers used for amplification
AIP56 promoter	Phdp AIP56 putative promoter region obtained by PCR amplification (373bp)	5'TAAAACGAATTACACCAAGTACCATCCATCTTGTAATGATTTAGAATTAATT CAAGCTGAATTGGTGAGAAATGTGGAGATTAATCATCTCTTCGGTAATAATGT GTCATTATTAATGATTAAGAATTGTATGAAGCCATGAGTGACAGTGTGTTGTG TTTACTGTTAAATATTGGTATCTATAAATCAGATCTTAAATAGGACGATATTAA GATAATAAAGTATACATATCGGAAAGTTATTTAGCGTGCAAGTGATATATAAA ACACAAACAAGTCGTTTGTATCTACAACTTACGATTTGGATGCTTTTTCTCTATT TATTAAAAACGGTATATTAACAGGATGTCACAGTGAAAAAATACTCAATAAT C 3'	promAIP56_smaI_F 5' CGCCCGGGTAAAACGAATTACACCAAGT 3' promoAIP56_TAT_R 5' ATTAGTGAAGTTATCCATGATTATTGAGTATTTTTT 3'
PBT promoter	Phdp PBT putative promoter region obtained by PCR amplification (353bp)	5'GGTGATAATTAACATATTCATTATCAAGTAATATATCATTTATTTCTGATGTG GATACATGAATAAAATAATGTATCAAAATGTAATGGGTTGTATCAACTCAATA TCAATATTGCCTTTAGTTTATGACAATAAAATACATGTAGCTTAAATGCAATGA ACAAGCTTGTATTTTGATGTTTTTGTAGAAAATAGCACTAAATTTATAATTTAA TTTGGTGCTATATGCTAAGTTGATAATTTTTAATTGAATCAATAAGAATCCTTG TTTTTACAATTAAGGAGGTAATGATATTTAATAATAGTGCAAAACAGAAGTTC CAAATTTTAATAATCATATTAATGTTATGGAGC 3'	PromPTB_FW 5' GGTGATAATTAACATATTCATTATCAAG 3' PromPTB_RV 5' CTCCATAACATTAATATGATTATTAAAATTTGGT 3'
PnpA promoter	Phdp PnpA putative promoter region obtained by PCR amplification (480bp)	5'TCGAATTTAAGGTACAAGACATTTTATAACTTCAGGAATAATAAAGGACTAT CCACTTTACCTGTCTTGTCCCCCTACATAATGAGATCGTTTACACAAATTAGCA AATATAAATAATTACATTTCATTACAATTTACATTCTAAAAATATAGCGTCTTT TTATAAAGATCTTATTTATTGGAATGGAGGTCACAATAAATAGAACAGTTCTAA TATTGCATCCCCGTAAGGAATATGATAAAACTGTTATTACATAATAAACTCAA ATAAAACCTCTCTTAACAGTAATTAACAATATATTTAAGTAAAAATATCAATTT ATGGCAATATCAATCTCAATATTGCTTTACCTAATAAGAGATATTATCCAAAG ATAGAATTAGTATTCTCACGTAGATAAAGGGAAATTCATGAATATAAATAAA CATTTAATGCTATTAGCATTATTAACCAACTATAGTTATGCAAATGGAAACAA CA 3'	promoter_NLPC_F 5' TCGAATTTAAGGTACAAGAC 3' promoter_NLPC_R 5' CTGTTGTTTCCATTTGCATAA 3'
OMP19 promoter	Phdp OMP19 putative promoter region obtained by PCR amplification (250bp)	5'CGTGGCTCAATGAGCAATTAATGCAAAAATAATCTTACGGGGATAAGTACA TAATCGCGACGAATAATTACATTAAAGCACATTAATGCGACTTACCTTTTTGCT TCTGTCATCTACACTGTGTTCAGTTAATAAAACAGTGTGTTTATTTTTTATTTGT GATTCCGTCATAAAAAGTAAGGTAAGAGATGATGAAGAGTATGAAAGGTCTA TTGATTGTTGTTGGTGTACTAAGTTCTTTGGTGTGTGG 3'	Promotor_OMP19_FW 5' CGTGGCTCAATGAGCAATTAATGC 3' Promotor_OMP19_RV 5' CCACACACCAAAGAACTTAGTACACC 3'
PLA promoter	Phdp PLA putative promoter region obtained by PCR amplification (231bp); Negative control for EMSA identified by qRT-PCR in Phdd, conserved in Phdp	5'GGCCAAGGCCGTAATAAACCTGCTGGACAAAAACCGACCAGCAAATTTAGC GGTAAGCCAAAAAACAAACGATAGTATAAAACTCGTTACATAAATAAATTTA TAGCGCTGAACAATTTCTTTTGTCAGCGCTATTTTTTTACATAACCTTTAAGCTT TTTGCTCAATTTTCAGTAGAATAGCGATAACGCCAATCGATCCATGGGTTTATT AAAAAGGATTACTCACTCT 3'	FW_PLA 5' GGCCAAGGCCGTAATAAACCTGCTGG 3' RV_PLA 5' AGAGTGAGTAATCCTTTTTAATAAACCC 3'
PAD A (ATAV16) promoter	Phdp HV10 strain PAD A putative promoter region obtained by PCR amplification (574bp); Promoter used for complementation in MT1415	5'GCGGATCCCTTCGTTACAGCCATTAGGGAAGATCTAACTAAAATCTGGCAA AACACCAAAAACAGTATAGAAAACGCTCAAAAGTAACCTGTTTTAGTAGGCT AAGTTATAAGAAAGACGGTTAATGATTGATTTTTAAGTGTTATTGTCAGAGTG GTTAGAAATTGAAATTCCTAACCATCAAGGTCAAAAAATAACCTTAACGTACA ATAATTTTCGATATCCAAACTGACCTCTGTATAGCCTCATGACGAGCTGTGCGA GGAATACCAAGCTCGCGTAGCGATATCATCACCAACCCTTCTAACGAGTGATA TAGCCTCTTATTTCACTATATTTACCCCATACTCTTTCCCTTCGTCCTCCTAAGCG CTCTTTTGCTGTGGTTGATATAAGTAAATAGGGTGATTGTCGTATGACAAAAG GAAGAAATCAGAAGGACTCAAGTCAAATTGTAGACACTTTGCAGACGAAAAC TTGACATATAGATGAGATAAATTACTTCAATATATTCTAAGTGTGATTTAACTT TCAAAACCACTATAAAATAACTAAGGTAAGTTAAAGATAATGC 3'	comp ATAV16 fwd 5' GCGGATCCCTTCGTTACAGCCATTAG 3' promATAV16_RV 5' GCATTATCTTTAACTTACCTTAGTTATTTTATAGTGG 3'
PAD B (ATAV17) promoter	Phdp HV10 strain PAD A putative promoter region obtained by PCR amplification (247bp); Promoter used for complementation in MT1415	5'GGATCCTGGTTTGTCTGGGTGCATAGACAGGAAGATACCTGTCTATGCCTGT TATGAACAGTAAAACTAACAGGTCGTTAGTTGCTGCCGTAGGCAGCCTATGTT CTAACCCTTAGTAGACATAACATAGACACTTACATGCAATAACTTACTGTAGT CTTTTTGAAACCTTAATTTATTCTTATCGCGTATTTAAGAGAAAGAATACGAAT GCATATTTATAAATAAGGTTTTAGATTATGAAC 3'	comp. ATAV17_fwd 5' GCGGATCCTGGTTTGTCTGGGTGCAT 3' promATAV17_RV 5' GTTCATAATCTAAAACCTTATTTATAAATATGC 3'